
# U.S. Freight Network Resiliency Analysis

Principal Investigators: Bruce Wang (TAMU), Yunlong Zhang (TAMU), Lee Han (UTK), Bo Zou (UIC)

Project Partners: Wal-Mart, Tennessee Department of Transportation, Oak Ridge National Lab

Report #FERSC-2023-Project1-1

Center for Freight Transportation for Efficient & Resilient Supply Chain (FERSC)

August 15, 2024

US Department of Transportation Grant 69A3552348338

Disclaimer

| 1. Report No. | 2. Government Accession No. | 3. Recipient's Catalog No. |
|---|---|---|
| **4. Title and Subtitle**<br>U.S. Freight Network Resiliency Analysis | | **5. Report Date**<br>August 15, 2024<br>**6. Performing Organization Code** |
| **7. Author(s)**<br>Bruce Wang (TAMU) ORCID: 0000-0003-0645-273X, Yunlong Zhang (TAMU) ORCID: 0000-0003-2404-5409, Lee Han (UTK) ORCID: 0000-0002-1381-1254, Bo Zou (UIC) ORCID: 0000-0003-4485-5548 | | **8. Performing Organization Report No.**<br>FERSC-2023-Project1-1 |
| **9. Performing Organization Name and Address**<br>Center for Freight Transportation for Efficient & Resilient Supply Chain (FERSC)<br>UT Center for Transportation Research<br>309 Conference Center Building<br>Knoxville TN 37996-4133 | | **10. Work Unit No.**<br>**11. Contract or Grant No.**<br>69A3552348338 |
| **12. Sponsoring Agency Name and Address**<br>US Department of Transportation<br>Office of the Secretary of Transportation–Research<br>1200 New Jersey Avenue, SE<br>Washington, DC 20590 | | **13. Type of Report and Period Covered**<br>Annual report: 9/1/2023–8/15/2024<br>**14. Sponsoring Agency Code**<br>Office of the Secretary of Transportation-Research |

**15. Supplementary Notes**
Conducted in cooperation with the U.S. Department of Transportation, Federal Highway Administration.


**16. Abstract**
The freight system is a complex, interconnected integration of subsystems—including ports, highways, and critical infrastructure like bridges—all of which are potentially vulnerable to various disturbances, such as extreme weather events or structural fractures. This project is a collaboration between TAMU and UTK, focusing on the analysis and enhancement of U.S. freight network resilience. TAMU's effort, enhancing port resilience to impending tropical cyclones by estimating impact rankings with a deep recommendation algorithm, focuses on alleviating the impact of tropical cyclones on port operations, while UTK's effort, freight network resilience in response to infrastructure failures, focuses on analyzing the impact of infrastructure failures on the surface transportation system.

In Part I, we enhance port impact estimation by focusing on ranking impacts rather than predicting them, as the latter tends to be unreliable. Using a comprehensive dataset of interactions between ports and cyclones, we adopted deep recommendation algorithms to estimate the impending impact of cyclones on ports. In the retrieval phase, ten ports potentially affected by an impending cyclone are identified through a rule-based filter. Then, three recommendation algorithms with data augmentation are employed in the ranking phase. Trained on data from 2017 to 2021 and tested with Hurricanes Nicole and Ian in 2022, Wide & Deep Learning effectively identifies impacted ports and achieves the desired ranking performance, particularly for the most affected ports. This framework enables improved prioritization of resources and response planning ahead of impending cyclones to mitigate potential impacts on freight systems.

Part II investigates the resilience of the U.S. freight network by analyzing the impacts of the 83-day closure of the Hernando De Soto Bridge in Memphis, Tennessee, which occurred from May 11 to July 31, 2021, due to a structural fracture. The research aims to quantify the effects of this critical infrastructure disruption on freight movement, traffic patterns, and economic stability using a combination of methodologies, including a high-resolution truck volume estimation model and a comprehensive resilience evaluation framework. Results indicate significant shifts in traffic patterns, with increased congestion on alternative routes and notable economic consequences stemming from extended travel times and operational costs for freight carriers. The findings highlight the vulnerability of the U.S. freight network to single-point failures and emphasize the importance of redundancy in critical transportation links. This research provides essential insights for policymakers and transportation planners, informing strategies to enhance infrastructure resilience and mitigate the impacts of future disruptions on freight movement and economic stability.


| 17. Key Words | 18. Distribution Statement |
|---|---|
| Freight System; Disturbances; Tropical Cyclones; Infrastructure Failure; Data-Driven; Resilience | No restrictions, available through the National Technical Information Service, Springfield, VA 22161. |

| 19. Security Classif. (of this report) | 20. Security Classif. (of this page) | 21. No. of Pages | 22. Price |
|---|---|---|---|
| Unclassified | Unclassified | | |

# Table of Contents

# Executive Summary

The economic stability of the United States relies heavily on an extensive freight transportation network that spans highways, railways, ports, and other interconnected routes. This network facilitates the movement of goods essential to domestic and international markets. However, the system is vulnerable to disruptions, where an interruption can quickly led to widespread delays, increased costs, and inefficiencies. Such vulnerabilities are especially pronounced at key infrastructure points, such as major ports and highway bridges, which act as critical connectors in the national supply chain. Ports, due to their coastal locations, face natural vulnerabilities to extreme weather events like tropical cyclones. Meanwhile, bridges, critical links in the freight network, are also concerning; currently, 7.5% of U.S. bridges are structurally deficient, jeopardizing freight transportation reliability as 178 million trips are made across these bridges daily (1–3). Therefore, this project aims to analyze critical nodes in the freight network with a focus on resilience and is composed of two major parts. The first part examines port system resilience in response to tropical cyclones, while the second part addresses the impact of bridge closures on freight networks.

Managing port operations effectively during tropical cyclones is crucial, yet existing methods struggle due to limited data and uncertain cyclone paths. To better understand port-cyclone interaction, the first part aims to develop a model to enhance port impact estimation before cyclone landfall. This analysis focuses on the Gulf of Mexico region from 2017 to 2022, considering 37 ports and 21 tropical cyclones. A Wide & Deep Learning (WDL) model is utilized to capture complex patterns while also memorizing specific feature interactions. Among the tested algorithms, the WDL model demonstrates superior performance by accurately identifying potentially impacted ports and providing reliable rankings, particularly for the most affected ports.

The second part examines the impact of this critical infrastructure disruption on freight movement and economic stability. The Hernando De Soto Bridge, a vital east-west transportation link across the Mississippi River, was closed for 83 days in 2021 due to a structural fracture. This closure significantly disrupted local, regional, and national freight operations, highlighting the vulnerability of the U.S. transportation network to single-point failures. Using a multi-faceted approach, the study analyzed traffic patterns, congestion levels, and economic impacts before, during, and after the bridge closure. Key findings reveal substantial changes in traffic flow, increased congestion on alternative routes, and significant economic consequences due to extended travel times and operational costs. The study also provides insights into the adaptability of the freight network and the time required for normal operations to resume.

Through examining port vulnerabilities to natural hazards and the effects of bridge closures on freight mobility, the project highlights how critical infrastructure disruptions can trigger cascading economic impacts. By developing predictive models and analyzing past events, this project informs strategies that enhance resilience, improve impact forecasting, and support a stable and efficient freight network essential for economic growth.

# Part I: Enhancing port resilience to impending tropical cyclones by estimating impact rankings with a deep recommendation algorithm

## Problem Description

The maritime transportation is a critical component of the freight system in the United States. According to statistical data from the Bureau of Transportation Statistics (BTS), approximately 69% of goods traded by the U.S. are shipped through waterways, primarily utilizing seagoing vessels (4). More than 95% of all U.S. trade relates to maritime transport, and vessels move around $11.4 trillion worth of products in and out of U.S. ports annually. Global warming and climate change pose significant challenges to maritime transportation, with rising sea levels and increasingly severe weather events impacting operational efficiency and reliability (5,6). Ports, essential nodes in the supply chain that connect maritime routes to trucks, trains, and barges, are particularly vulnerable. Located in coastal areas, they face heightened risks from flooding, hurricanes, and storms, which can cause delays, operational disruptions, and infrastructure damage (7,8).

Although machine learning (ML) and deep learning (DL) have become widely adopted in maritime transportation due to the abundance of AIS data and advancements in data-driven methods (9–11), their performance under extreme weather conditions remains limited. Most studies focus on regular operations, predicting metrics like estimated time of arrival and port throughput. However, extreme weather events, such as tropical cyclones, introduce complexities often overlooked due to two major challenges: the rarity of such events results in insufficient data, limiting model training, and the complexity of port operations during severe weather is difficult to capture within typical analytical frameworks. Although, Li et al.,(12) made an initial step toward providing a dataset for port resilience research by integrating comprehensive AIS data and cyclone records in the Gulf of Mexico (2017-2020), and innovatively applying recommendation algorithms to model the complex interactions between tropical cyclones and port operations. Their approach remains a preliminary attempt. The study does not fully leverage the potential of machine learning to address these complex challenges.

Therefore, this study aims to address these challenges by developing a deep learning-based framework to estimate port performance during tropical cyclones. Rather than relying solely on factorization machines (FM) to capture second-order feature crossings, we employ a more advanced method to capture higher-order feature crossings. This approach enhances the model's ability to represent complex relationships between cyclones and port operations, leading to a more accurate assessment of port impact. This part is designed to provide prioritized recommendations for emergency response and resource allocation, assisting port authorities and vessel operators in minimizing disruptions in the face of an impending hurricane (13).

## Approach

A dataset of cyclones and port vessel counts is applied in this study, with detailed information on 37 ports and 21 tropical cyclones in Gulf of Mexico from 2017 to 2022 that represent the interactions between ports and cyclones (12). For the purposes of our analysis, the study utilizes the 2022 data as

the testing dataset. Due to limited amount of data for training, especially for DL models, we proposed innovative data argumentation methods based on the properties of spaghetti models for cyclone trajectories. In this study, for each hurricane, we generate ten random landfall locations as input, assuming a uniform distribution along the coastline within the forecasting uncertainty cone. This approach assumes that the actual landfall location is equally likely to occur anywhere along the coastline within the cone, and these generated locations are used to replace the actual landfall location. Through this data augmentation (shown in **Figure 1**), we can enhance the robustness of the recommendation algorithm and estimate a more accurate port impact ranking under forecasting uncertainty (14). For each tropical cyclone, ten different potential landfall locations are generated, yet the number of impact days remains constant across these variations.

Consequently, this approach yields a dataset of 15,540 records (37 ports × 21 tropical cyclones × 20 potential landfall locations), representing the interactions between ports and cyclones. For analysis, we designate 2022 data as the testing set, while data from 2017, 2018, 2019, and 2021 serve as the training set. Our contribution lies in applying machine learning and deep learning-based recommendation algorithms to capture complex, higher-order feature interactions relevant to port impact under cyclones. Through a rigorous comparison of candidate models, we identify the most effective approach, offering port authorities a refined tool to enhance decision-making in disaster scenarios. Further details are provided in the methodology section.

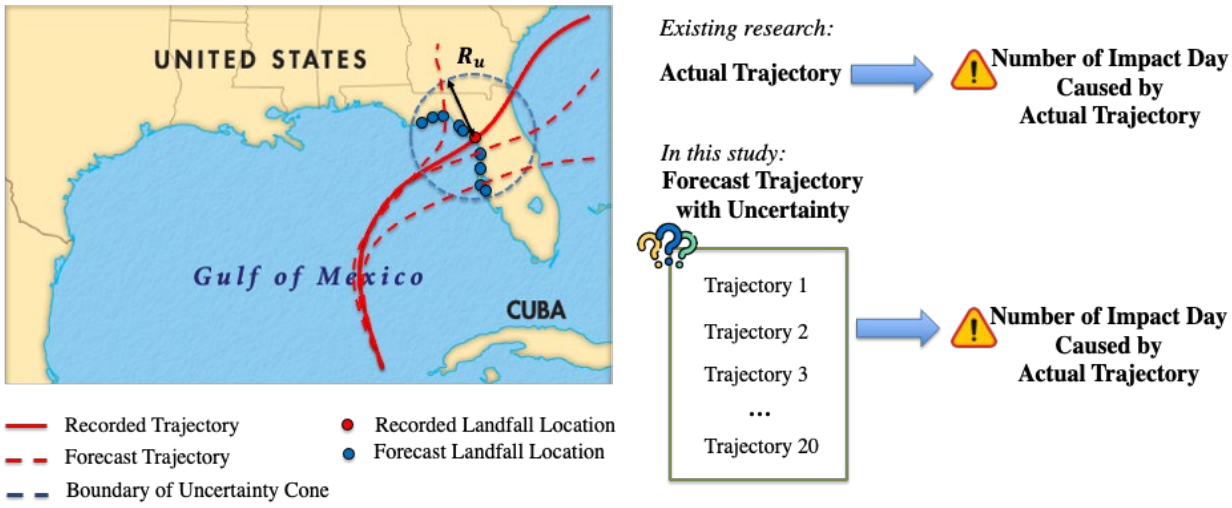


**Figure 1. Illustration of data augmentation**

## Methodology

The cornerstone of recommendation algorithms is their capacity for feature crossing, a process that combines multiple attributes to capture the complex interactions between ports and cyclones. This capability is crucial for conducting accurate and nuanced estimations, as it allows algorithms to consider not only individual features but also the interaction between them. Different algorithms employ various approaches to feature crossing, ranging from second-order interactions to higher-order interactions, as well as ensemble methods that combine multiple approach (15). For example,

FM model the interactions through second-order feature crossings. They adeptly capture interactions between pairs of features, uncovering hidden patterns that might not be apparent from examining individual features alone (16). Additionally, the Gradient Boosting Decision Trees (GBDT) combined with linear regression (LR) is utilized to further enhance the modeling of high-order interaction. For more advanced modeling, DL-based method (17) are employed.

We utilize the WDL framework, which combines the modeling power of neural networks with the broad reach of linear models. This approach allows for handling higher-order feature interactions and capturing complex patterns within the data, enhancing predictive accuracy in assessing port impacts under cyclonic events. Additionally, the FM and GBDT models are applied as benchmarks to evaluate and compare model performance.

**Factorization Machine**

FM is a ML algorithm that efficiently captures second-order feature interaction by factorizing the interaction matrix, making it well-suited for handling sparse and high-dimensional data in the recommendation system (16). Compared to linear models, FM can model second-order feature interaction through factorization of the interaction matrix into latent vectors. Therefore, FM is able to estimate interactions even with extremely sparse data. Note that the input of FM can be only categorical features. To generate the second-order interaction terms, we have discretized the continuous features into categorical measures using the 25th, 50th, and 75th percentiles in the same way as (18,19).

In FM, the model is combined with a linear regression component and feature interaction component, as in **Eq. (1)**. However, it will simultaneously increase the computational complexity due to the interaction components. To mitigate this, FM model the feature interaction using latent factors $v$. Each feature $x_i$ has a latent factor $v_i$ of size $k$ (i.e., hyperparameter), and two features' interaction are modeled as $\langle v_i, v_j \rangle = \sum_{f=1}^{k} v_{i,f} v_{j,f}$, where $\langle \cdot \rangle$ is the dot product of the two latent factors. Finally, the number of parameters for the interaction term reduces from $n^2$ to $n \times k$. Introducing matrix $\boldsymbol{V}$ is similar to factorizing the original weight matrix of the interaction term.

$$\hat{y}(\boldsymbol{x}) = \underbrace{w_0 + \sum_{i=1}^{n} w_i x_i}_{\text{linear regression}} + \underbrace{\sum_{i=1}^{n-1} \sum_{j=i+1}^{n} \langle v_i, v_j \rangle x_i x_j}_{\text{interaction}} \quad (1)$$

Where $w_0$ is the bias term and $w_i$ is the weight corresponding to feature vector $x_i$. To further reduce the time computational complex from $O(kn^2)$ in Eq. (1) to $O(kn)$, Eq. (1) can be rewritten as Eq. (2) in light of (16). In the end, we use a stochastic gradient descent (SGD) and least squares error to train FM in this study.

$$\hat{y}(\boldsymbol{x}) = w_0 + \sum_{i=1}^{n} w_i x_i + \frac{1}{2} \sum_{f=1}^{k} \left( \left( \sum_{i}^{n} v_{i,f} x_i \right)^2 - \sum_{i=1}^{n} v_{i,f}^2 x_i^2 \right) \quad (2)$$

**Gradient Boosted Decision Trees with Linear Regression**

Gradient Boosted Decision Trees (GBDT) is capable of effectively learning non-linear relationships from input features (20,21). Unlike their application in typical classification tasks where GBDT maps directly between inputs and outputs, in recommendation systems, GBDT plays a distinct role in feature generation. Specifically, the paths through the decision trees create high-order features through the conjunction of conditions at each decision node. These embedded outputs are then utilized to train a linear regression model to estimate and rank the impacts of cyclones on different ports. The process begins by initializing the model with an initial estimation that minimizes the loss function, typically the squared error for regression. The GBDT model is trained iteratively, with each tree fitting the residuals $r_i^m$ of the previous model, progressively refining the estimations and capturing complex patterns (22). This iterative refinement acts as supervised feature embedding, transforming the input features into a compact, binary-valued vector. For example, **Figure 2(a)** illustrates five distinct paths, each defined by decisions at split nodes, which are optimized to minimize the loss function. Each path represents a high-order feature interaction. For instance, the first path might embed the condition: "hurricane wind scale ≠ H5 AND harbor type ≠ seaport AND distance from the port to the forecasted landfall location is less than 200 km". If an input feature satisfies this condition, the corresponding output variable will be set to 1. Otherwise, it will be 0. These feature crossing are embedded into a binary vector where the dimensionality is determined by the number of paths across all trees. This embedded feature set is then used as input for linear regression, which optimizes weights and biases to further minimize the squared error. This method leverages the strengths of both GBDT and linear regression: GBDT captures complex non-linear interactions, while linear regression offers a scalable and interpretable framework for modeling these interactions. The pseudocode in **Table 1** and framework illustration in **Figure 2(b)** outline the integration of GBDT with linear regression.

**Table 1. Pseudo code for GBDT with LR**

**GBDT with Linear Regression**

**Input:** Training dataset $\{x_i, y_i\}_{i=1}^N$ Number of tree ($T$), Depth of each tree ($D$), learning rate ($\eta$), Loss function ($L(\cdot)$)

**Output:** Estimated impact

Initialize GBDT model $M_0(x)$ as $F_0(x) = \text{argmin}_\gamma \sum_i L(y_i, \gamma)$

**For** $t \leftarrow 1$ to $T$:

  Compute Residuals: $r_i^t = -\left[\frac{\partial L(y_i, F_{t-1}(x_i))}{\partial F_{t-1}(x_i)}\right]_{F_{t-1}(x_i)}$

  **Train Decision Tree** $h_t(x)$ **to residuals** $r_i^m$ with a maximum depth $D$

  **Update GBDT Model** $M_t(x) = M_{t-1}(x) + \eta h_t(x)$

**end for**

**For** $i \leftarrow 1$ **to** $N$ **do**

  $\phi(x_i) = OneHotEncode(\{h_1(x_i), \ldots h_T(x_i)\})$

**end for**

**Train Linear Regression** $\hat{y} = \boldsymbol{w}^T \boldsymbol{\phi}(\boldsymbol{x}) + b$

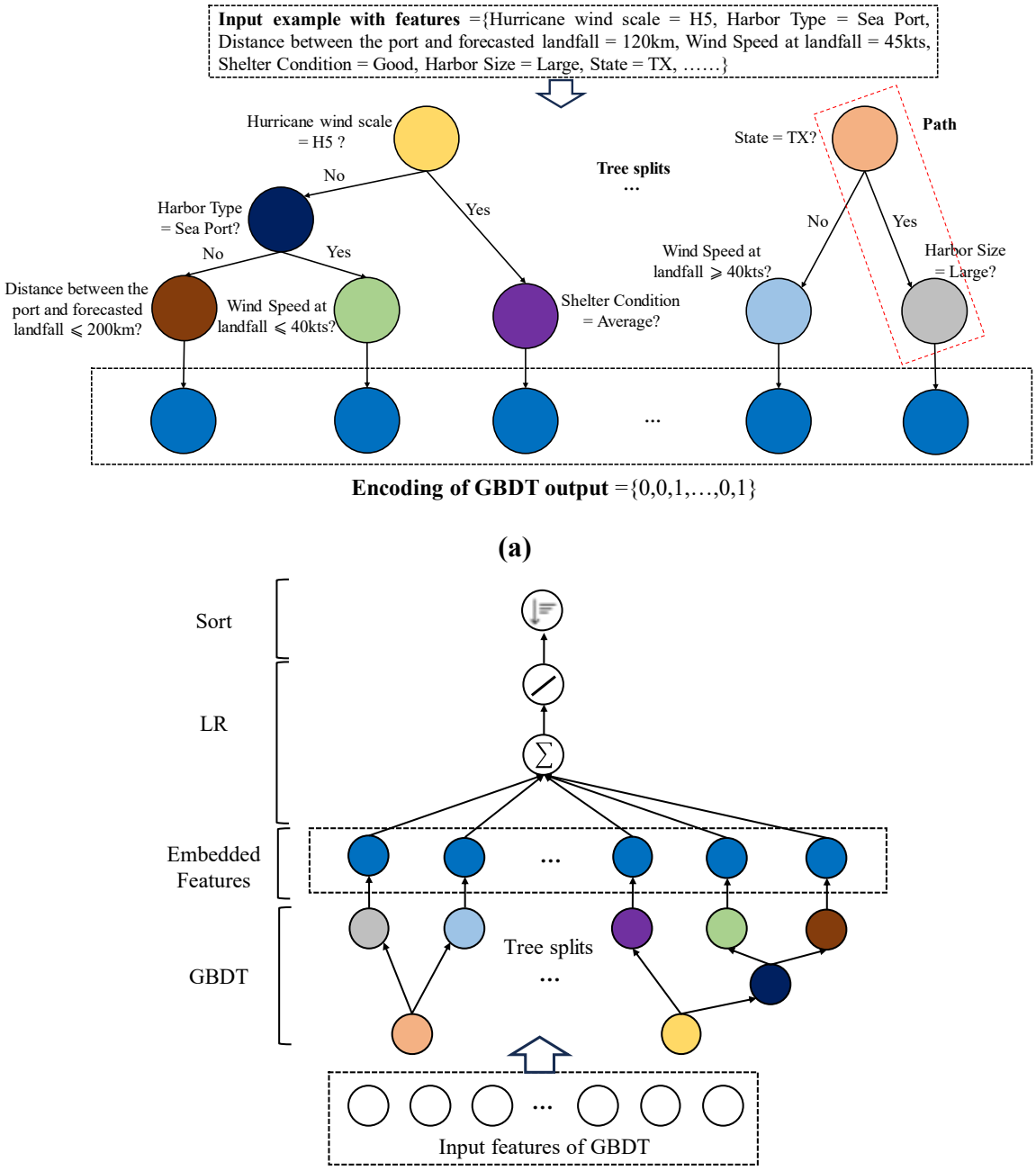


**Figure 2. Example of GBDT embedding (a) and Algorithm framework of GBDT with LR (b)**

### Wide & Deep Learning

FM excel at managing sparse data and efficiently modeling pairwise interactions, but it is mainly limited to linear relationships between input and output. GBDT+LR tackles more complex, non-linear interactions between port and tropical cyclone. In this approach, GBDT is used to embedding the

input features, which LR then uses for estimation and ranking the impact. While effective, this sequential combination leads to a disconnect between feature generation and estimation, hindering the ability to refine feature generation based on the estimation results. To address these limitations, we introduce WDL, an end-to-end model that combine the advantages of linear models, such as FM, with deep neural networks (DNN). The wide component of the Wide and Deep Learning (WDL) model focuses on memorization, using sparse data to effectively capture frequent patterns. This ensures it quickly recognizes and utilizes key features that appear often in historical interaction between port and cyclone, enhancing stability and relevance in estimation. The deep component of the WDL model uses DNNs to effectively generalize complex, nonlinear interactions and uncover intricate pattern in the data through dense embeddings. This capability allows WDL to perform well on previously unseen pattern, enhancing model's adaptability and robustness. The embedding vector are randomly initialized and then optimized during back propagation in the training process to minimize the loss function. These dense embedding vectors are then fed into the hidden layers of the neural network during forward propagation. Specifically, each hidden layer is implemented as in Eq. (3).

$$a^{(l+1)} = f(W^{(l)}a^{(l)} + b^{(l)}) \tag{3}$$

Where $l$ is the number of layers, $f(\cdot)$ is the activation function, typically ReLUs. $a^{(l)}$, $W^{(l)}$, and $b^{(l)}$ represent the output of activation function, weight, and bias for the $l^{th}$ hidden layer, respectively. The deep component processes feature through multiple hidden layers and non-linear activation functions, learning complex high-order interactions. The final estimation result from WDL is given by Eq. (4) and the WDL network structure is shown in **Figure 3**.

$$\hat{y}_{WDL}(x) = w_{wide}^{T}[x, \phi(x)] + w_{deep}^{T}a^{(l_f)} + b \tag{4}$$

Where $\hat{y}_{WDL}(x)$ is the ranking score. $\phi(x)$ are the cross-product transformations of the original features $x$, as the same in the interaction term in **Eq. (1)**, and $b$ is the bias term. $w_{wide}$ is the vector of all wide model weights and $w_{deep}$ refer to the weight in the final activation output $a^{(l_f)}$. To prevent the overfitting, $L_2$ regularization could be used to penalize larger weight in the model.

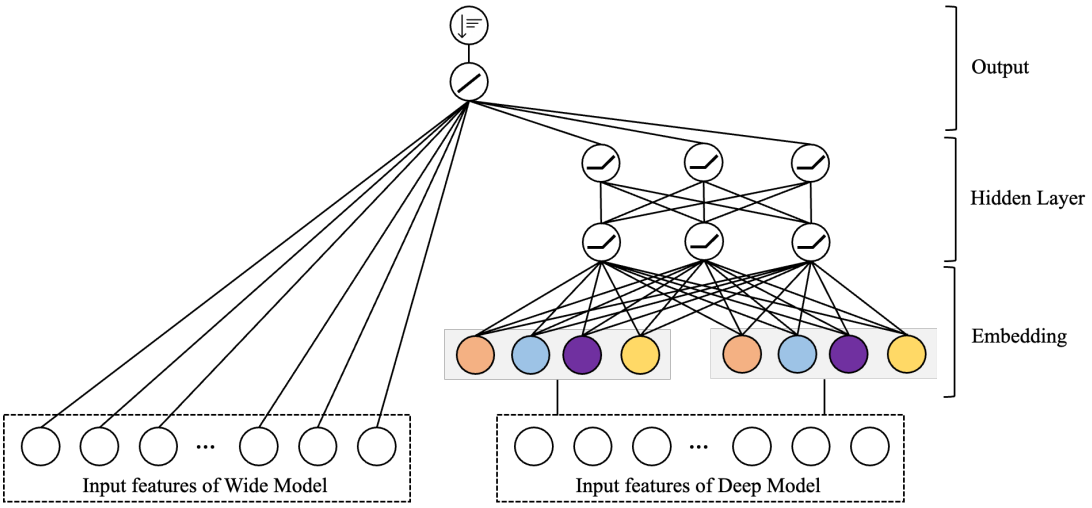


**Figure 3. Network of Wide & Deep Learning**

## Findings

To comprehensively evaluate the proposed recommendation algorithm for port impact ranking, data from 2017 to 2021 (excluding 2020) are used for training, while Hurricane Ian and Hurricane Nicole from 2022 is used for the testing dataset. The hurricane-related features for input are based on the forecast hurricane trajectory rather than the actual trajectory. As described in the methodology, in order to evaluate the sensitivity of the model to hurricane landfall uncertainty, we randomly generate 20 landfall locations from the intersection of uncertainty cone of impending hurricane and coastline, as input. An ideal method shall balance performance and robustness, in other words, the model shall perform desirably considering the uncertainty of the forecast hurricane trajectories. Note that 20% of the training data is set aside solely to form the validation dataset to prevent overfitting. In this study, the Python packages PyFM, Scikit-Learn, and PyTorch are utilized to construct the FM, GBDT+LR, and WDL models. The fine-tuned hyperparameters are listed in **Table 2**.

**Table 2. Hyperparameters setting in the recommendation algorithms**

| Parameters | Setting |
|---|---|
| ***FM*** | |
| Dimensionality of factorization ($k$) | 100 |
| Initial learning rate | 0.001 |
| ***GBDT+LR*** | |
| Number of tree ($T$) | 120 |
| Depth of each tree ($D$) | 30 |
| learning rate ($\eta$) | 0.05 |
| ***WDL*** | |
| Layer number and units in each layer of DNN | (256, 128, 64) |
| $L_2$ regularize strength for wide part | 10e3 |

| | |
|---|---|
| Batch size | 256 |
| Epochs | 100 |
| Validation split ratio | 0.2 |
| Optimizer | Adam |

Moreover, a distance-based method is selected to be the baseline algorithm in this study, which calculates the impact based on the distance from the landfall location to the port. The distance-based method is intuitive and widely used in real-life scenarios. A port is considered impacted by tropical cyclones if it falls within the radius of tropical cyclones, with severity of the impact increase as the port's proximity to the landfall location decreases (23). Based on the definition of the hurricane strike cycle from NHC (2023), the radius of the strike cycle is around 75 nautical miles (around 140 km). Considering the secondary disaster of tropical cyclones, including flooding and heavy precipitation, we extend the radius to 400 km, centered on hurricane's landfall location. Thus, if the distance of a port to the landfall location or nearest point of the cyclone is less than 400 km, the distance-based method assumes that the port is impacted by the specific tropical cyclone. The severity of the impact is ranked according to the distance, with closer distances indicating more severe impacts. Although this method is relatively coarse, it is similar to how state governments announce mandatory and voluntary evacuations (25,26) making it a reasonable choice for a baseline.


**Figure 4. Illustration of distance-based method**

### Performance Measures

The proposed recommendation algorithm framework consists of two key steps: retrieval and ranking, as illustrated. In the retrieval step, potentially impacted ports in the Gulf of Mexico are selected based on a rules-based filter. Subsequently, the ranking step employs the trained algorithms from the training step (i.e., FM, GBDT+LR, and WDL) to rank the impact on ports under each tropical cyclones,

based on the estimated number of impact days. The retrieval step essentially serves as a classification to determine if the port will potentially be impacted by the impending cyclone. To assess classification performance, we employed metrics including precision, recall, and the F2 score. For the ranking phase, metrics including mean absolute error (MAE), root mean square error (RMSE), and rank biased overlap are utilized to evaluate the performance of regression and ranking tasks.

Considering the adverse impact of cyclones on ports, precision and recall are prioritized over accuracy because impacted ports are the minority class. This focus ensures that the model effectively identifies truly impacted ports while minimizing false negatives, which are instances where impacted ports are mistakenly classified as unimpacted, crucial for effective disaster response. Precision measures the proportion of the top $L$ ports estimated that are actually impacted, and recall is the proportion of all the ports actually impacted that are correctly identified, as shown in **Eqs. (5)** and **(6)**. Both measures range from 0 to 1, and a higher value indicates a better performance.

$$\text{precision} = \frac{|U \cap L|}{|L|} \tag{5}$$

$$\text{recall} = \frac{|U \cap L|}{|U|} \tag{6}$$

Where $U$ is the set of actually impacted ports, and $L$ represents the set of top ports identified to be impacted by impending cyclones. Here, we set the $|L| = 10$ for the recommendation algorithms. $|\cdot|$ represents the size of a set. To balance these metric, F-beta measure, specifically the F2-score is adopted, because it prioritizes recall, ensuring the most impacted port are correctly identified, even if precision is sacrificed.

$$F_\beta = \frac{(1+\beta^2)\times\text{recall}\times\text{precision}}{(\beta^2\times\text{precision})+\text{recall}} \tag{7}$$

In the ranking step, we rank the port impact for the top $L$ ports based on the estimated number of impact days. Therefore, MAE and RMSE are used to evaluate the regression performance, as shown in **Eqs (8)** and **(9)**.

$$MAE = \frac{1}{N}\sum_{i=1}^{N}|y_i - \hat{y}_i| \tag{8}$$

$$RMSE = \sqrt{\frac{1}{N}\sum_{i=1}^{N}(y_i - \hat{y}_i)^2} \tag{9}$$

Where $y_i$ and $\hat{y}_i$ represent the actual and estimated number of impact days, respectively. However, this study focuses more on the ranking performance. Due to the complex interactions between ports

and cyclones and the limited dataset, the performance of estimating the exact number of impact days may not be desired. Rank-Biased Overlap (RBO) is used to assess the similarity between two ranked lists, offering a detailed evaluation of a model's ability to accurately rank impacted ports.

$$RBO = (1-p)\sum_{d=1}^{D} p^{d-1} \cdot \frac{|U_{1:d} \cap L_{1:d}|}{d} \quad (10)$$

Where $D$ is the depth of the list $L$, which indicates the position or rank within the ranked list. $p$ is the hyperparameter from 0 to 1. A smaller $p$ value gives more weight to higher ranked items. In this study, several ports share identical rankings because they have the same number of impact days. To manage these ties effectively, we set the $p$ value as 1, ensuring uniform weighting across rankings and addressing the issue of ties (27). The RBO, ranging from 0 to 1, reflects ranking accuracy, with higher values indicating better performance.

**Results**

In the framework of the recommendation algorithm, the rule-based filter in the retrieval step is consistent. Therefore, it was assessed alongside the baseline method, as shown in **Figure 5**. recommendation algorithm's precision is lower than that of the distance-based method for both testing hurricanes because of its more conservative approach, assuming that the top 10 nearest ports to the landfall are impacted. In contrast, the distance-based method considers only ports within 400 km of the landfall as impacted. Despite its lower precision, the recommendation algorithm. Take Hurricane Nicole as an example, there are four impacted ports, for the top 10 ranked list of which the highest precision for FM-based method is 0.4 (i.e., 4/10). While it has a lower precision compared to the distance-based method, it already achieves the upper-performance threshold and exhibits a relatively higher recall. This higher recall indicates that the framework can effectively capture as many impacted ports as possible, enabling port authorities to mitigate potential economic losses due to unpreparedness and inadequate planning. In terms of the comprehensive metric – the F-2 measure – the average performance of the recommendation algorithm outperforms the distance-based method. Importantly, the recommendation algorithm exhibits lower performance variance compared to the distance-based method, demonstrating greater robustness against the uncertainty of cyclones forecasting. This suggests that the data augmentation approach is effective. It is noted that the best performance of certain metrics, like the F-2 measure during Hurricane Nicole, is higher with the distance-based method than with the recommendation algorithm. This indicates that when hurricane trajectories are accurately forecasted, the distance-based method could be more effective. However, considering the inherent uncertainties in forecasting and the importance of reliability in disaster management, the recommendation algorithm is generally more desirable for estimating the impact of impending cyclones on port operations.

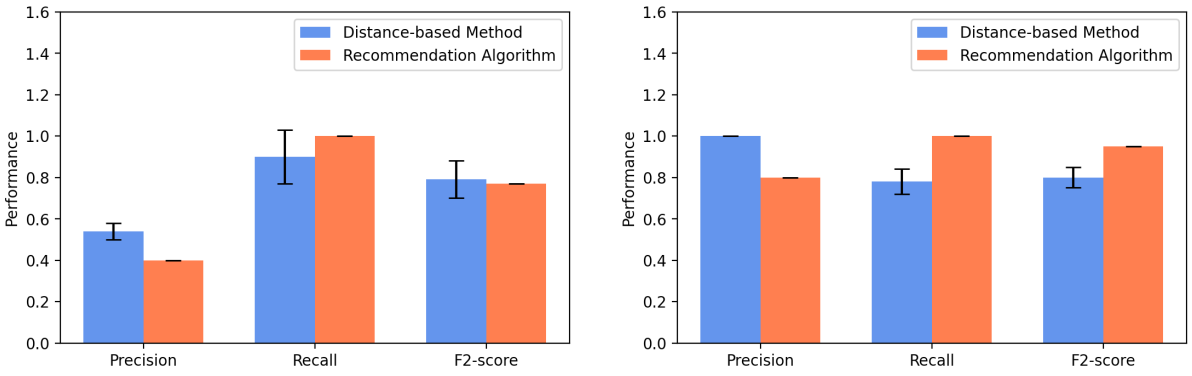


(a) Nicole (b) Ian

**Figure 5. Classification performance between baseline and recommendation algorithm**

### Comparison of Ranking Performance

The distance-based method only provides impact rankings and does not estimate number of impact days, making MAE and RMSE metrics inapplicable. In the testing hurricanes, regression performance improved sequentially from FM to GBDT+LR to WDL, demonstrating the progressively enhanced ability of second-order, higher-order, and ensemble feature crossing approaches to capture the intricate interactions between ports and cyclones. However, this does not guarantee corresponding improvements in ranking performance. For example, the RBO for the higher-order model GBDT+LR did not surpass that of the second-order model FM and was even worse than the distance-based method. GBDT+LR excels in regression by capturing complex, non-linear relationships with its ensemble of decision trees, and linear regression fine-tunes these estimations to precise number of impact day. However, its linear component struggles with ranking tasks, focusing on minimizing estimation errors rather than maintaining the correct ranking. Conversely, FM effectively models interactions across all features, which is crucial for accurately preserving the order in ranking tasks. This capability enables FM to perform better in evaluations like RBO that prioritize the quality of ordering, highlighting why GBDT+LR, despite its accuracy in regression, falls short in ranking performance compared to FM. The WDL model excels in both regression and ranking due to its hybrid structure that combines a wide linear model with a deep neural network. The wide component efficiently captures feature interactions, aiding in accurate ranking by prioritizing feature importance. Meanwhile, the deep component models complex, non-linear relationships, enhancing regression performance by generalizing well on diverse data inputs. Similar to its classification performance, the recommendation algorithm demonstrates greater resilience to forecasting uncertainty in cyclones, showing more consistent performance in both regression and ranking, as indicated by its smaller variance.

**Table 3. Comparison of model ranking performance**

| Model | MAE | RMSE | RBO |
|---|---|---|---|
| *Hurricane Nicole (H1)* | | | |
| Distance-Based | / | / | 0.454 (0.112) |
| FM | 1.346 (0.048) | 1.743 (0.073) | 0.682 (0.027) |
| GBDT+LR | 0.498 (0.013) | 0.802 (0.012) | 0.440 (0.050) |
| WDL | 0.477 (0.028) | 0.691 (0.021) | **0.842 (0.025)** |
| *Hurricane Ian (H5)* | | | |
| Distance-Based | / | / | 0.607 (0.090) |
| FM | 1.004 (0.088) | 1.301 (0.111) | 0.723 (0.023) |
| GBDT+LR | 0.915 (0.001) | 1.180 (0.002) | 0.682 (0.001) |
| WDL | 0.871 (0.036) | 0.933 (0.020) | **0.944 (0.011)** |

Notes: The value in the bracket is the standard deviation for each performance metrics under potential landfill location.

To better demonstrate the ranking performance of recommendation algorithm, we randomly selected two potential hurricane trajectories for Hurricanes Nicole and Ian within the uncertainty cone, and we have detailed their estimated port impact rankings in **Tables 4** and **5**. The WDL method consistently and effectively ranks impacts under forecasting uncertainty, particularly excelling at identifying the top-ranked ports in actual impacts. The shortcomings of the distance-based method become more pronounced with longer forecast durations, which tend to increase forecasting errors. Specifically, the estimated port impact become unreliable, especially with extended forecast durations (e.g., 96-hour forecasting). If the ports around the Gulf prepare based on these unreliable estimates some ports may over-prepare while others under-prepare, both of which can increase safety risk and economic losses. The proposed recommendation algorithm not only effectively identifies impacted ports but also precisely rank the impact of impending cyclone on ports. This capability ensures more accurate preparedness and response, mitigating risks and potential economic losses.

**Table 4. Comparison of estimated port impact ranking and actual ranking under Nicole**

| Port Rank | Actual Impact | Distance-based 1 | Distance-based 2 | Distance-based 3 | WDL-based 1 | WDL-based 2 | WDL-based 3 |
|---|---|---|---|---|---|---|---|
| **1** | Miami | Canaveral | PlamBeach | Canaveral | Miami | Miami | Miami |
| **2** | PalmBeach | PlamBeach | Everglades | PlamBeach | PlamBeach | PlamBeach | PlamBeach |
| **3** | Evergaldes | Tampa | Miami | Everglades | Manatee | Manatee | Manatee |
| **4** | Jacksonville | Manatee | Canaveral | Tampa | Jacksonville | Mobile | Jacksonville |
| **5** | \ | Everglades | Mantatee | Manatee | Mobile | Jacksonville | Mobile |
| **6** | \ | Jacksonville | Tampa | Miami | Everglades | Everglades | Everglades |
| **7** | \ | Miami | \ | Jacksonville | Pascagoula | Pascagoula | Pascagoula |
| **8** | \ | \ | \ | \ | Panama | Panama | Panama |
| **9** | \ | \ | \ | \ | Canaveral | Canaveral | Canaveral |
| **10** | \ | \ | \ | \ | Tampa | Tampa | Tampa |

**Table 5. Comparison of estimated port impact ranking and actual ranking under Ian**

| Port Rank | Actual Impact | Distance-based 1 | Distance-based 2 | Distance-based 3 | WDL-based 1 | WDL-based 2 | WDL-based 3 |
|---|---|---|---|---|---|---|---|
| **1** | Everglades | Miami | Manatee | Manatee | Everglade | Everglade | Everglade |
| **2** | Miami | Everglades | Tampa | Tampa | Miami | Miami | Miami |
| **3** | Manatee | PlamBeach | Everglades | Everglades | Manatee | Manatee | Manatee |
| **4** | Tampa | Manatee | Miami | PlamBeach | Tampa | Tampa | Tampa |
| **5** | PlamBeach | Tampa | PlamBeach | Canaveral | PlamBeach | Canaveral | Jacksonville |
| **6** | Jacksonville | Canaveral | Canaveral | \ | Canaveral | PlamBeach | PlamBeach |
| **7** | Panama | \ | \ | \ | Jacksonville | Jacksonville | Canaveral |
| **8** | Canaveral | \ | \ | \ | Pascagoula | Pascagoula | Panama |
| **9** | \ | \ | \ | \ | Mobile | Mobile | Pascagoula |
| **10** | \ | \ | \ | \ | Panama | Panama | Mobile |

# Part II: Freight network resilience in response to infrastructure failures

## Problem Description

The economic stability of the United States relies heavily on an extensive freight transportation network that spans highways, railways, ports, and other interconnected routes. This network facilitates the movement of goods essential to domestic and international markets. However, the system is vulnerable to disruptions at critical points, where an interruption can quickly lead to widespread delays, increased costs, and inefficiencies. Such vulnerabilities are especially pronounced at key infrastructure points, such as major river crossings, which act as critical connectors in the national supply chain. Disruptions in these areas can severely impact freight transport, delaying shipments and increasing costs that ultimately affect businesses, consumers, and the broader economy.

The Hernando De Soto Bridge, a six-lane steel-tied arch structure on Interstate 40, has been an essential transportation link since its completion in 1973. This bridge facilitates east-west interstate truck traffic across the Mississippi River, connecting West Memphis, Arkansas, with Memphis, Tennessee. Alongside the nearby I-55 bridge, it is one of only two crossings of the Mississippi River in the Memphis area. Each day, the I-40 bridge supports over 42,000 vehicles, including more than 13,700 trucks, underscoring its importance to national commerce, transportation, and defense.

The Memphis region, located near the New Madrid Seismic Zone, has historically experienced significant seismic activity, including major earthquakes in the early 19th century. Recognizing the potential for future seismic events, the Tennessee Department of Transportation (TDOT) and the Arkansas Department of Transportation (ARDOT) initiated a seismic retrofit of the I-40 bridge in the early 1990s. This project aimed to enhance the bridge's resilience against earthquakes, fortifying its foundations and other structural elements to withstand a magnitude 7.7 earthquake. The retrofit further enables the bridge to serve as a critical post-earthquake route for emergency vehicles and the general public.

On May 11, 2021, a structural inspection revealed a fracture in a key steel support beam of the I-40 bridge. This discovery prompted an immediate closure of the bridge, halting both vehicular traffic and river navigation beneath it to safeguard public safety. Following a thorough investigation and repair process, the eastbound lanes of the bridge were reopened on July 31, 2021, with the westbound lanes following on August 2, 2021.

Despite the relatively brief 83-day closure, the I-40 bridge's temporary shutdown disrupted local, regional, and national transportation and freight operations. This disruption highlighted the critical nature of the bridge for U.S. infrastructure and renewed interest in exploring the feasibility of constructing an additional or replacement crossing over the Mississippi River in this region.

**Figure 6** shows the location of the I-40 bridge over Mississippi River. This bridge is a vital component of the U.S. freight network, carrying thousands of trucks daily as they move goods across the country. Because of its central location and its role as one of the primary river crossings in the region, any prolonged closure or structural failure of this bridge would have severe consequences. Such a

disruption could force trucks and other freight to take extended detours, leading to significant delays, increased fuel costs, and congestion on alternative routes. The resultant delays could interrupt supply chains, increase costs for businesses, and create shortages, all of which could ripple through the national economy.

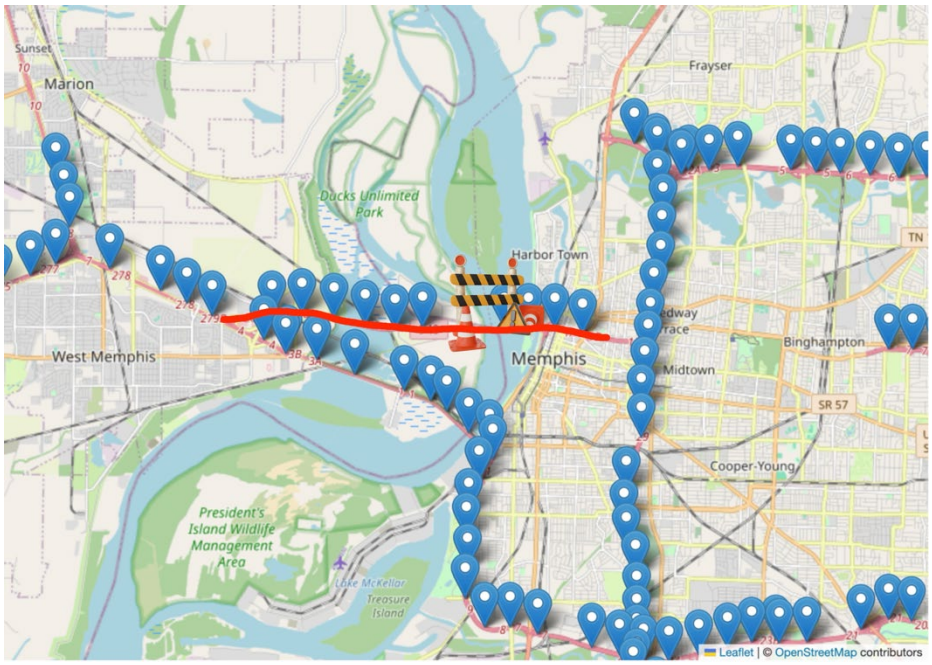


**Figure 6. Location of Hernando De Soto Bridge**

Understanding the effects of a potential disruption to the Hernando de Soto Bridge is essential to strengthening the resiliency of the national freight network. By examining how the bridge functions within the larger freight system and identifying potential weaknesses, researchers can provide insights into how a closure might affect transport routes, travel times, and costs. This study aims to quantify these impacts, providing a detailed assessment of how disruptions influence the flow of goods and the economy as a whole. Specifically, this research will examine the logistical and economic effects of a simulated closure, analyzing how freight routes adapt and what financial impacts arise from increased transit times and operational costs. Such an analysis is crucial for developing strategies to mitigate these effects, improving the resilience of the U.S. freight network and reducing the risk of economic strain from future disruptions.

Past research has explored various aspects of infrastructure resilience, including studies on how transportation networks respond to inclement weather, infrastructure failures, and increased demand. Previous models have often provided general assessments of network disruptions but have not always focused specifically on freight movement at critical junctures like the De Soto Bridge. Additionally, existing models may lack the data resolution needed to capture the real-time impacts of a bridge closure on freight operations accurately. This study builds on previous work by narrowing the focus to a key infrastructure component and enhancing data analysis to improve precision in understanding impacts.

The primary objectives are to assess current freight flow models and identify any gaps that may limit the understanding of a disruption's impact on national and regional scales. This approach involves

detailed analysis of traffic patterns, identifying alternative routes, and evaluating the associated economic costs. With this foundation, the study aims to develop a comprehensive framework for assessing and preparing for potential disruptions to essential freight infrastructure, thus contributing to a more robust and adaptable national transportation system.


**Figure 7. Summary of Part II**

## Approach

This section details the approach taken to evaluate the resilience of the U.S. freight network in response to infrastructure failures, with a specific focus on the case of the Hernando de Soto Bridge closure. Recognizing the critical role that this bridge plays as a major east-west transportation route across the Mississippi River, this study aims to understand how its prolonged closure impacted freight flow, detour routes, congestion levels, and logistical costs. Through this case study, the project seeks to identify and quantify patterns of response within the freight network under significant infrastructural disruption, with the ultimate goal of informing future resilience strategies.

The Hernando de Soto Bridge, connecting Memphis, Tennessee, and West Memphis, Arkansas along Interstate 40, experienced an unexpected closure from May 11, 2021, to July 31, 2021, following the discovery of a structural fracture. This bridge serves as a critical connection point for the region, supporting substantial daily freight traffic vital to regional and national supply chains. The abrupt loss of this corridor led to immediate detours, rerouting freight and other traffic through alternative crossings, which in turn increased congestion and travel time on surrounding infrastructure. By analyzing this event, the study aims to provide insights into how infrastructure failures at strategic nodes impact the freight network and test the network's resilience to significant disruptions.

To deepen the analysis, a new method was adopted to quantify the resilience of the traffic network by examining the statistical distribution of congestion levels across different phases of the bridge

closure. Specifically, the study assessed attributes such as the frequency and duration of extreme congestion events, with particular attention to prolonged delays. This approach enabled a detailed understanding of how frequently and to what extent severe traffic congestion occurred, providing insight into the network's ability to absorb and dissipate traffic surges during periods of heightened strain. By analyzing these statistical attributes, the study could better quantify network resilience by capturing how quickly typical conditions resumed and identifying thresholds where congestion duration could lead to substantial freight delays and economic impacts.

To accomplish this, the approach combines real-world data acquisition with a structured analysis of traffic patterns and freight movement before, during, and after the bridge closure. By extending the analysis beyond the closure period itself, the study is able to capture baseline traffic patterns, assess immediate responses to the disruption, and observe the gradual return to typical conditions. Through this temporal segmentation, the project can identify critical shifts in traffic flow and congestion levels attributable to the bridge closure, as well as any lasting impacts on the freight network.

The study's design also prioritizes data integrity and comprehensiveness. A wide range of data sources were collected, including traffic flow, travel times, and freight-specific movement data, to enable a nuanced and detailed understanding of the disruption's impacts. The following sections outline the assumptions made, scope of analysis, study area specifics, study duration, and the data acquisition process. These components together define a robust framework for assessing the resilience of the freight network in response to the Hernando de Soto Bridge closure and provide a foundation for extended analysis in subsequent project phases.

**Assumptions**

To conduct a systematic and effective analysis of the bridge closure, a set of key assumptions guided the approach:

1. **Traffic Rerouting**: It is assumed that the traffic typically crossing the Hernando de Soto Bridge was redirected to other river crossings such as I-55 during the closure, causing increased congestion and extended travel times on nearby alternate routes.
2. **Temporal Phases**: The study assumes distinct changes in traffic flow across three temporal phases: pre-closure, closure, and post-closure. These phases serve as comparative benchmarks to assess fluctuations in congestion and freight movement, thereby enabling a precise assessment of the disruption's impact and the network's recovery.
3. **Data Integrity**: The data sources utilized were assumed to provide a comprehensive view of traffic volumes and travel times, although potential limitations in data resolution and completeness were taken into consideration during analysis.

**Scope**

This analysis focuses on the effects of the Hernando de Soto Bridge closure on freight transport and traffic conditions within the Memphis area. As a first-year effort, the study aims to quantify the immediate impacts of the closure, including shifts in traffic flow, increases in congestion, and rising operational costs for freight carriers. Though centered on the Memphis region, this study's findings

intend to inform broader resilience assessments for critical infrastructure within the U.S. freight network.

The scope of this phase includes the following objectives:

1. Identifying and analyzing changes in traffic and congestion patterns due to the bridge closure.
2. Quantifying the delays, detours, and additional logistical costs associated with the disruption.
3. Establishing a baseline dataset for future, extended analyses within the multi-year project.

**Study Area: Memphis Region**

The study area encompasses the Memphis metropolitan region, which serves as a major logistics hub with extensive freight activity. The Hernando de Soto Bridge on Interstate 40, which crosses the Mississippi River, is a critical transportation corridor within this region. By analyzing this specific area, where the bridge's closure led to significant rerouting of traffic, the study provides a focused assessment of the disruption's local effects, while offering insights into broader network resilience. Additional crossings and highways in the surrounding area were also included to evaluate the impacts of redirected freight traffic during the bridge's closure.

**Study Duration**

The study period spans from **March 1, 2021, to September 30, 2021**, capturing data for two months before the closure, the duration of the closure itself (from **May 11, 2021, to July 31, 2021**), and a subsequent period to observe post-closure traffic patterns. This extended study period allowed for a comprehensive assessment of traffic conditions before, during, and after the incident, providing a clearer understanding of both the immediate impacts and the eventual resumption of normal traffic patterns within the Memphis area.

**Data Acquisition**

To support an in-depth analysis, this study placed a significant emphasis on data acquisition, collecting multiple datasets to enable a well-rounded examination of the bridge closure's impacts:

- **TDOT Radar Detection System (RDS)**: Detector-based traffic volume data from the Tennessee Department of Transportation provided a baseline of typical traffic volume conditions in the Memphis area, crucial for evaluating changes due to the bridge closure.
- **National Performance Management Research Data Set (NPMRDS)**: This dataset included travel time and speed information, enabling an assessment of congestion levels and travel time reliability throughout the study period.
- **WAZE Data**: Data from the community-driven WAZE application offered real-time traffic and congestion insights, enhancing the ability to detect shifts in traffic patterns and congestion levels during the bridge closure.
- **EROAD Data**: This dataset, provided by Robinsight in collaboration with Oregon State University, tracks approximately 40,000 trucks within the Pacific Northwest, offering aggregated truck trip data to analyze freight movement patterns. However, with a penetration rate of just 0.31% relative to the estimated 13 million trucks operating in the U.S., the dataset's low coverage limits its representativeness for a study focused on the Memphis area. Additionally, EROAD data rounds truck trip counts to the nearest 50, which

reduces the precision necessary to capture specific fluctuations in freight traffic. While EROAD data adds valuable freight-specific insights, these limitations in sample size and data precision create challenges for accurately assessing the broader impacts of the Hernando de Soto Bridge closure on the national freight network.

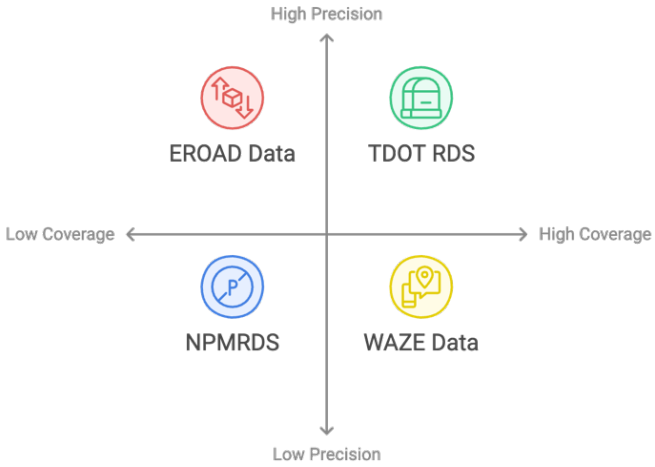


**Figure 8. Data Acquisition for this Study**

As shown in **Figure 8**, the data collection process required close coordination with relevant agencies to ensure the timely acquisition of each dataset. All data underwent rigorous quality assurance checks, including data validation, wrangling, and restructuring, to ensure accuracy and compatibility for subsequent analysis. This extensive preparation facilitated a seamless integration of multiple data sources, forming a comprehensive foundation for the study's analysis.

**Multi-Year Effort**

This analysis represents the first phase in a multi-year initiative aimed at developing a more resilient freight infrastructure model across the United States. Given the complexity of the U.S. freight network, subsequent phases of the project will build on the foundational insights gained during this study. This initial analysis of the Hernando de Soto Bridge closure provides essential data for understanding network responses to disruptions, serving as a preliminary study for ongoing efforts to enhance national freight resilience in the face of potential future challenges.

## Methodology

This section provides an overview of the technical frameworks employed in this study to evaluate the impact of the Hernando de Soto Bridge closure and to assess the resilience of the U.S. freight network in response to infrastructure disruptions. Two main frameworks underpin the analysis: a high-resolution truck volume estimation model and a comprehensive resilience evaluation model.

The first and essential component of this methodology is the truck volume estimation framework (28). This model allows for detailed analysis of freight volume across both spatial and temporal dimensions, offering an enhanced view of truck movement patterns. By providing granular data on volume shifts and congestion levels, this framework supports the identification of changes in freight routes, bottlenecks, and redistribution of traffic flow resulting from the bridge closure. For a full understanding of the technical aspects, readers are encouraged to refer to the original paper (28) as specific details are omitted here for brevity.

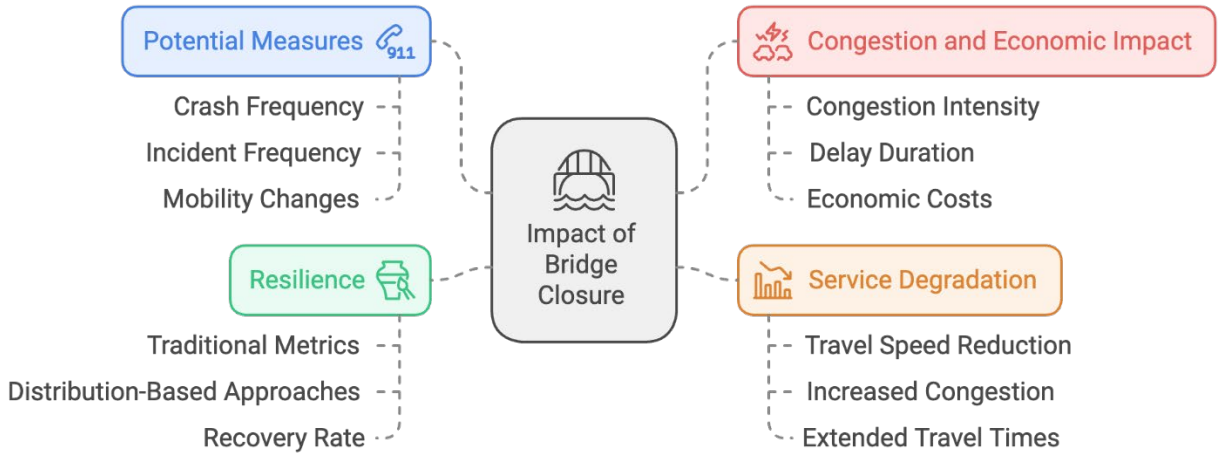


**Figure 9. The Comprehensive Resilience Evaluation Model**

The second framework employed is the resilience evaluation model, which assesses the adaptability and recovery of the freight transportation network in the face of disruption. This model integrates both the traditional resilience triangle and a series of targeted investigations across four key areas:

1. **Potential Measures (Crash, Incident, Mobility)**: This aspect examines the frequency of crashes and incidents on alternative routes and assesses changes in overall mobility due to the traffic rerouting caused by the bridge closure. By evaluating these indicators, the study captures safety and operational challenges that arose during the disruption period.
2. **Congestion, Delay, and Economic Impact**: Here, the analysis focuses on the intensity of congestion, duration of delays, and the associated economic impacts. Quantifying these factors reveals the immediate consequences of the closure for both freight carriers and the general public, providing insights into the broader economic costs of infrastructure vulnerability.
3. **Quantification of Service Degradation**: This aspect measures the extent to which service levels on affected routes declined during the closure. By analyzing reductions in travel speed,

increases in congestion, and extended travel times, this metric provides a quantitative assessment of the service degradation experienced by freight and passenger vehicles.

4. **New Definitions and Measures of Resilience**: Finally, resilience is defined in terms of the network's capacity to absorb, adapt, and recover from disruptions. The model uses both traditional resilience triangle metrics and innovative distribution-based approaches to measure resilience, offering a comprehensive view of how the transportation network responds over time. This includes evaluating both the immediate disruptions and the rate at which normalcy is restored.

In combination, these frameworks allow for a robust analysis of the Hernando de Soto Bridge closure's impact on freight operations and contribute to a broader understanding of transportation network resilience in response to infrastructure challenges.

Assessing the resilience of a transportation system, particularly in the context of disruptions such as the Hernando De Soto Bridge closure, involves applying quantitative resilience measures to capture various stages of the system's response. These resilience measures describe the system's state prior to disruption, quantify the extent of performance degradation, assess the recovery rate, and estimate the time required for full restoration to normal operations. This comprehensive view of resilience is essential for stakeholders, including transportation planners and policymakers, to make informed decisions on network design, pre-event planning, disaster relief, prioritization of capacity expansion, and maintenance (29).

In urban highway networks, resilience is often measured using multiple quantitative metrics rather than a single universal measure. Researchers have proposed a range of metrics, including those related to delay, capacity, speed, travel time, and cost, to assess resilience in urban highway networks (30–32). The selection of these measures can vary depending on the type of disruption, transportation mode, modeling approach, and specific study objectives, reflecting the complex nature of transportation systems and their varied responses to different types of stressors.

As resilience in transportation networks remains an emerging research area, there is ongoing debate about whether a standard set of resilience measures will eventually be agreed upon by practitioners. Some researchers (33,34) advocate for using a multi-metric approach to capture the diverse aspects of resilience. Others (30,35) have experimented with combining several measures into a composite index to provide a more holistic assessment. These approaches underscore the need for flexibility in resilience metrics, as different disruptive events and network types may require unique measurement approaches.

In light of these considerations, this study employs a combination of traditional and innovative resilience measures:

1. **Resilience Triangle**: This traditional approach quantifies resilience by assessing the area under the performance curve over time, capturing the extent and duration of service loss and recovery following the disruption.

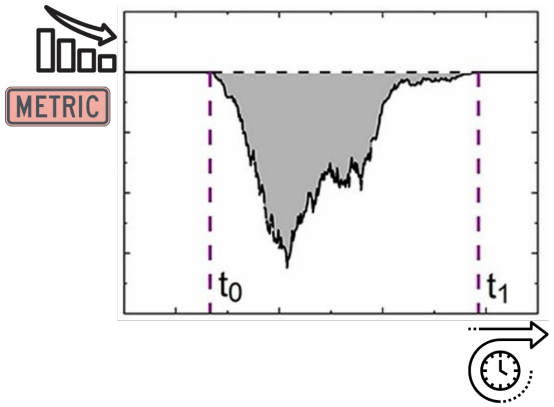


**Figure 10. The Traditional Resilience Triangle**

As shown in **Figure 10**, the resilience is often defined as

$$R = \frac{\int_{t_0}^{t_1} P(t)}{(t_1 - t_0)P_0}$$

, where P is any performance metric of the system, $t_0$, the time when the disruptive event occurs, and $t_1$, the time when the system reaches full recovery.

The resilience triangle diagram illustrates the degradation and recovery of system performance over time following a disruptive event. The y-axis represents the performance metric (or system functionality), with higher values indicating optimal performance. The x-axis represents time, with two marked points.

In this diagram:

- Initial Performance (pre-disruption) is represented by the horizontal line at the top.
- Disruption Impact causes a rapid drop in performance, forming the left side of the triangle.
- Recovery Phase shows the gradual improvement in performance until it stabilizes near its original level.
- Shaded Area represents the total performance loss during the disruption and recovery phases, illustrating the resilience "gap."

The resilience triangle visually quantifies resilience as the system's ability to reduce the area of performance loss and speed up recovery, ultimately aiming to minimize disruption impacts and restore normal operation as quickly as possible.

In the context of traffic resilience, the recovery period begins as measures are taken to resolve the disruption (e.g., clearing the accident scene, adjusting signal timings, or implementing detours). During this phase, traffic performance gradually improves until it reaches a stable post-recovery state close to its pre-disruption level.

In traffic resilience terms, the shaded area represents the cumulative traffic performance loss due to the disruption. This area captures both the extent and duration of the disruption's impact on traffic flow.

In our case, the resilience can be interpreted by looking at the shaded area in the following way:

High Traffic Resilience: A highly resilient traffic network would have a small shaded area, indicating that the system either experiences minimal degradation or recovers quickly. For example, a network with alternative routes and responsive traffic management can quickly mitigate the disruption.

Low Traffic Resilience: A less resilient traffic system would show a larger shaded area, meaning a significant loss in performance for an extended time. This could happen in networks without robust incident management strategies, resulting in prolonged congestion and delays.

2. **Distribution Analysis**: Rooted in the theoretical framework (36), this advanced approach examines congestion metrics such as the duration, length, and area of congestion events, which often follow a long-tail distribution. By analyzing these distribution patterns, the study can gain deeper insights into both frequent minor disruptions and rare but severe events, offering a more granular understanding of resilience in transportation systems (36).

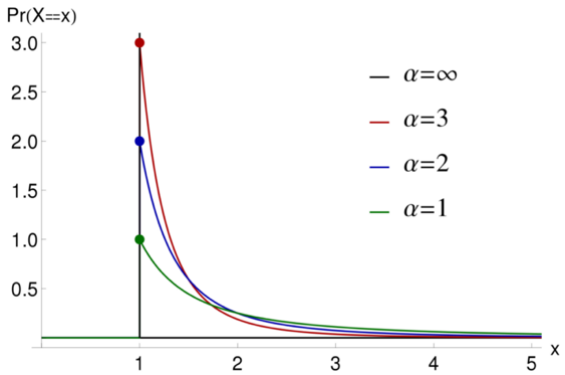


**Figure 11. The Power-law/Pareto Distribution**

For a variable $X$, which could represent congestion duration, congestion length, or congestion area, the **long-tail or the Pareto distribution** is given by:

$$P(X > x) = \left(\frac{x_{min}}{l}\right)^{\alpha}$$

where:

- $x$ is the threshold value of interest for the congestion variable.
- $x_{min}$ is the minimum threshold beyond which the power-law behavior applies (e.g., a baseline congestion duration, length, or area for minor events).
- $\alpha$ is the tail exponent or shape parameter of the distribution,

For Congestion Duration ($X = T$): The distribution implies that most congestion events are short-lived, but there is a non-negligible probability of very long-lasting congestion.

For Congestion Length ($X = L$): Most congestion events are spatially limited, but rare events can affect extensive segments of the road network.

For Congestion Area ($X = D$): The area under the resilience triangle (indicating the cumulative impact of the congestion event) generally remains small, but a few events may cause severe, widespread performance loss. The area is often understood as the total delay (D) in traffic flow theory.

Note that the power law exponent $\alpha$ determines the "heaviness" of the tail:

he general form of the power-law distribution's probability density function (PDF) for a random variable X is:

$$f(x) = Cx^{-\alpha} \text{ for } x \geq x\_min$$

where:

$\alpha > 1$ is the tail exponent or shape parameter.

$x_{min}$ is the minimum threshold value beyond which the power-law behavior applies.

$C$ is a normalizing constant, typically $C = (\alpha - 1) \cdot x_{min}^{\alpha-1}$ for a continuous power-law distribution, ensuring that the total probability integrates to 1.

Impact of the Tail Exponent $\alpha$:

The tail exponent $\alpha$ determines the "heaviness" of the distribution's tail, meaning how likely the distribution is to produce very large values (i.e., extreme events):

When $\alpha$ is Close to 1:

- Heavier Tail: The distribution has a very heavy tail, which means that there is a high probability of large values, or extreme events. In a traffic context, this would mean a high likelihood of severe congestion events (long duration, large length, or large area).
- Example: For $\alpha$ = 1.1 , the probability of observing very high values of X (e.g., very long congestion) is significant, as the distribution decays very slowly. This results in a higher frequency of extreme congestion events.
- Infinite Mean and Variance: For $1 < \alpha < 2$ , the mean of the distribution diverges to infinity, and for $1 < \alpha < 3$ , the variance diverges. This indicates that the distribution is extremely variable, and the expected value of congestion duration, length, or area cannot be reliably calculated.

When $\alpha$ is Between 2 and 3:

- Moderate Tail: The distribution is still heavy-tailed but not as extreme as when $\alpha$ is closer to 1. Large values are still possible, but they are less probable than in distributions with smaller $\alpha$ .
- Finite Mean but Infinite Variance: For $2 < \alpha < 3$ , the mean of the distribution is finite, but the variance is still infinite. In traffic terms, while the average congestion duration or length is calculable, the variability is so high that extreme congestion events can still occur frequently, though less often than in cases with $\alpha < 2$ .

When $\alpha$ is Greater Than 3:

- Lighter Tail: The distribution has a lighter tail, meaning that extreme values are rare. Most observations will be closer to $x\_min$ , and large congestion events become increasingly uncommon.

- Finite Mean and Variance: For $\alpha > 3$, both the mean and variance of the distribution are finite, indicating a more predictable and less variable system. In traffic terms, congestion events are less likely to be extreme, so the system experiences fewer instances of prolonged or widespread congestion.
-

Interpretation of $\alpha$ in Traffic Congestion

- Smaller $\alpha$ (closer to 1): Indicates a system highly susceptible to extreme congestion events. The traffic network experiences frequent and severe disruptions, where the probability of extreme congestion (in terms of duration, length, or area) remains high.
- Moderate $\alpha$ (between 2 and 3): Implies a network where large congestion events can still happen, but they are less common. This might be seen in well-managed but complex networks where minor disruptions are common, and severe disruptions are possible but controlled.
- Larger $\alpha$ (greater than 3): Suggests a resilient traffic system where severe congestion events are rare. Most congestion events are mild and short-lived, and the probability of observing extreme events decreases rapidly.

Practical Use of $\alpha$ in Resilience Analysis

- Estimating $\alpha$ in empirical traffic data (e.g., historical records of congestion events) helps understand the likelihood and impact of extreme congestion events. A lower $\alpha$ indicates a need for targeted interventions to prevent or mitigate severe disruptions.
- By analyzing $\alpha$, traffic managers can:
- Design appropriate resilience strategies: Heavier-tailed distributions (smaller $\alpha$) suggest the need for robust incident management, alternative routes, and faster recovery protocols.
- Assess system performance improvements: A higher $\alpha$ after implementing resilience measures indicates that the system now experiences fewer extreme events, thus improving overall traffic resilience.

In summary, the tail exponent $\alpha$ **is a critical parameter in understanding traffic resilience**, as it dictates the frequency and impact of extreme congestion events. Lower values of $\alpha$ correlate with higher probabilities of severe, disruptive events, while higher values indicate a system with more stable and predictable congestion patterns.

The incorporation of multiple resilience measures in this study aligns with the evolving perspective in resilience research, recognizing that transportation networks are complex systems requiring a multi-dimensional assessment to capture their behavior under strain. This approach not only helps in understanding immediate impacts but also provides critical insights into the broader dynamics that inform recovery and long-term resilience planning.

## Findings

### Data documentation

The data used in this project primarily comes from two key sources: **RDS** data for traffic volume and **NPMRDS** data for travel times. These datasets were essential in understanding both the intensity of freight movement and the variation in travel times on affected routes before, during, and after the Hernando de Soto Bridge closure. However, the complexity and scale of the data required substantial efforts in data cleaning, restructuring, and imputation to ensure its quality and reliability for analysis.

First, **data cleaning** was crucial to eliminate inaccuracies and ensure consistency across datasets. This step involved removing outliers, handling erroneous records, and filtering out incomplete entries. For example, anomalous volume spikes in the RDS data and unusually high or low travel time entries in the NPMRDS data were identified and either corrected or excluded, based on comparison with adjacent data points.

**Restructuring** was another critical process to align both datasets for meaningful comparison. The RDS data provides traffic volumes at different locations, while the NPMRDS offers travel times across specific segments. To analyze them together, we reorganized the datasets into a compatible format, standardizing the temporal and spatial intervals so that traffic volume and travel time data could be synchronized across the same timeframes and locations. This restructuring allowed us to integrate volume and travel time data for comprehensive congestion and resilience analyses.

Given the incomplete nature of some entries, **data imputation** was performed to address missing values, especially in cases where travel times or traffic volumes were intermittently unrecorded. Imputation techniques, such as linear interpolation and Random Forest-based imputation, were applied to estimate missing values by referencing nearby data points with similar attributes. This imputation process was carefully managed to ensure that estimated values reflected realistic traffic patterns and did not introduce artificial trends.

These combined efforts in data cleaning, restructuring, and imputation established a robust and reliable dataset, providing the foundation for accurate analysis and assessment of the impacts of the Hernando de Soto Bridge closure on freight movement and network resilience.

### Analyses performed

The analyses performed in this study aimed to understand the impact of the Hernando de Soto Bridge closure on freight and passenger traffic, with a focus on detailed truck volume estimation, spatial and temporal congestion patterns, and resilience measures. Each analysis technique contributed to an understanding of the network's adaptability and recovery in response to the infrastructure disruption.

**1. Truck Volume Estimation**

The truck volume estimation analysis is foundational to our approach, allowing us to capture high-resolution data on freight movement patterns. This framework operates on a **30-second temporal resolution** and uses detectors spaced **0.5 miles apart** to estimate truck volumes. The primary inputs to this model are **speed, occupancy, and total volume** data collected at each detector

location. By analyzing these inputs, the model outputs an estimated truck count for each 30-second interval at each detector, providing a granular view of truck flow across key routes. This enhanced resolution enables precise tracking of changes in freight traffic density and flow patterns, especially along alternative routes used during the bridge closure. The 30-second, half-mile spaced data is particularly valuable for identifying bottlenecks and variations in freight activity, supporting a nuanced understanding of how truck routes adapted to the bridge closure.

**2. Space-Time Heatmap**

To visualize the spatial and temporal shifts in traffic congestion, we generated **space-time heatmaps** that illustrate congestion intensity over time across the study area. For example, **Figure 12** shows a heatmap for **July 2, 2021**, highlights congestion dynamics during a representative day within the closure period. These heatmaps use color intensity to indicate the level of congestion, with darker colors representing higher congestion levels. By displaying traffic speed in this way, we can observe how traffic queues evolved throughout the day, identifying peak times and locations where alternative routes experienced significant congestion spikes. This visual approach provides an intuitive understanding of the congestion distribution and supports further analyses of delay patterns and traffic impacts.

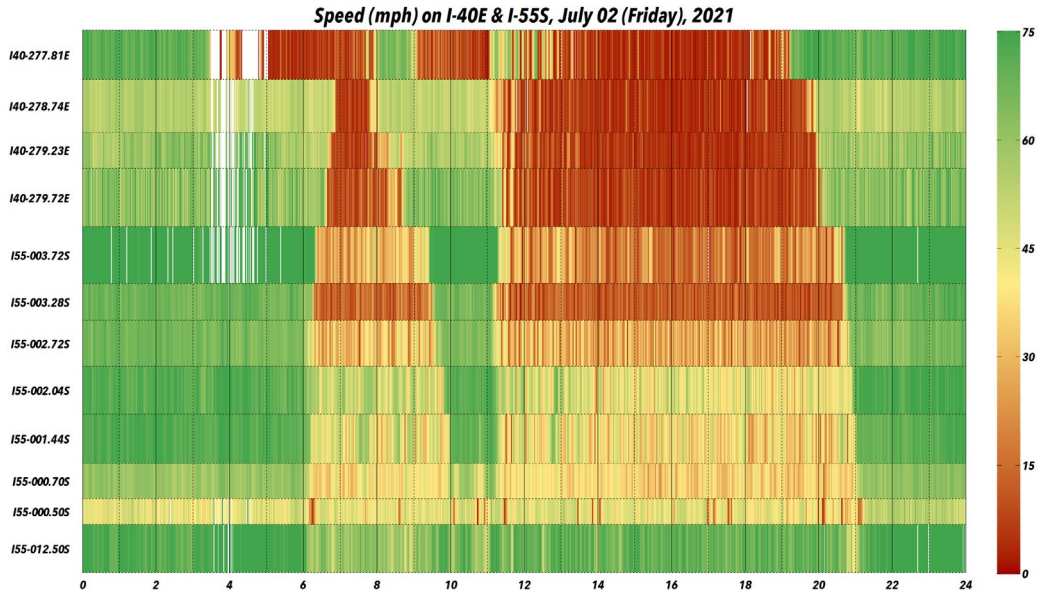


**Figure 12. Space-Time Diagram for Crossing-River Eastbound Traffic on July 2, 2021**

**3. Before/After Analysis**

To evaluate the impact of the bridge closure on different types of traffic, we conducted a **before/after analysis** that compared traffic patterns prior to, during, and after the closure. Separate analyses were performed for total traffic, passenger vehicles, and trucks, which enabled us to isolate the effects on freight traffic specifically. Metrics such as travel time, speed, and volume were compared across these time periods to identify shifts in traffic behavior and congestion levels. This comparison provides insights into how both freight and general traffic responded to the closure, revealing variations in route choices, delay impacts, and overall congestion changes.

**4. Measures of Resilience**

To assess the resilience of the freight transportation network, we applied a combination of **traditional resilience triangle metrics** and **distribution-based resilience measures**. The resilience triangle method evaluated the duration and intensity of service degradation and recovery, while the distribution-based method analyzed the statistical characteristics of congestion duration, particularly focusing on extreme congestion events. Metrics included crash frequency, incident rates, mobility impacts, congestion duration, and delay frequency. These measures allowed for a detailed quantification of the network's degradation and recovery trajectory, providing a nuanced understanding of how quickly and effectively the system adapted to and recovered from the disruption.

Through these analyses, we were able to assess both immediate impacts, such as congestion and delays, and longer-term resilience, such as recovery patterns and adaptations in freight routing.

### Before/After Analysis

**Figure 13** beblow illustrates the speed degradation across the entire Memphis area using average speed data from each detector. The timeline covers the critical period from May 11, 2021, to August 2, 2021, which coincides with the closure of the I-40 Hernando De Soto Bridge.

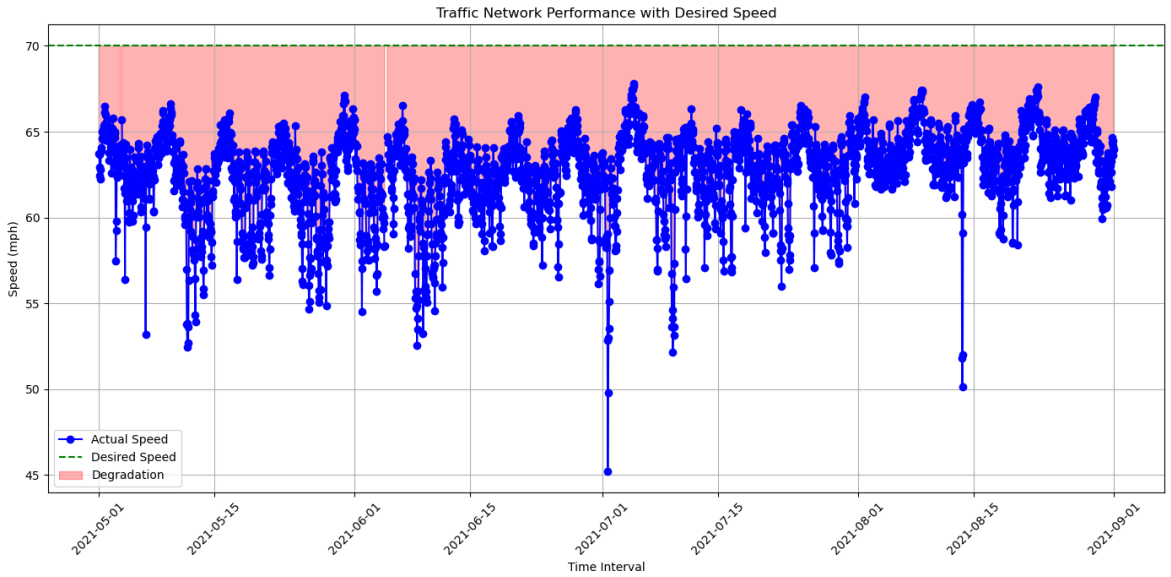


**Figure 13. Freight Network Performance Degradation by Speeds**

### Area-Wide Performance Stability:

Despite the disruption caused by the bridge closure, the figure shows that, on a regional scale, traffic performance remained relatively stable. The average speed across detectors hovers near the desired threshold, with frequent but contained dips into the degradation zone (red area). This suggests that while individual corridors experienced performance drops, the network as a whole managed to maintain a degree of stability.

### Localized Speed Degradation:

- While the area-wide performance shows stability, there are noticeable instances of speed degradation, as seen in the scattered dips below the desired speed. These dips likely correspond to localized congestion hotspots that arose from the redirected traffic load, particularly along alternate routes such as the I-55 bridge, which absorbed much of the rerouted traffic.
- The observed pattern reflects the network's adaptive capacity: despite increased pressure on certain corridors, the system managed to prevent widespread breakdowns, maintaining operational stability across Memphis.

**Implications for Resilience Assessment**:

This figure supports the case study by illustrating that the Memphis network demonstrated resilience under pressure, maintaining area-wide performance stability even with localized disruptions. This aligns with resilience metrics that measure the network's ability to "withstand, adapt to, and recover from" the bridge closure. Although specific routes faced congestion, the overall network avoided a system-wide degradation in performance.

In summary, the figure reveals that while the bridge closure created pockets of congestion, the Memphis area's traffic network sustained regional stability. This outcome reflects the network's resilience, a crucial factor in understanding its response to infrastructure failures. However, the performance stability seen in the area-wide average masks the intensified impact on the river-crossing corridors, specifically the I-55 bridge, which bore the brunt of rerouted traffic. The I-55 corridor experienced increased congestion and reduced speeds, underscoring the vulnerability of key river crossings during infrastructure disruptions.

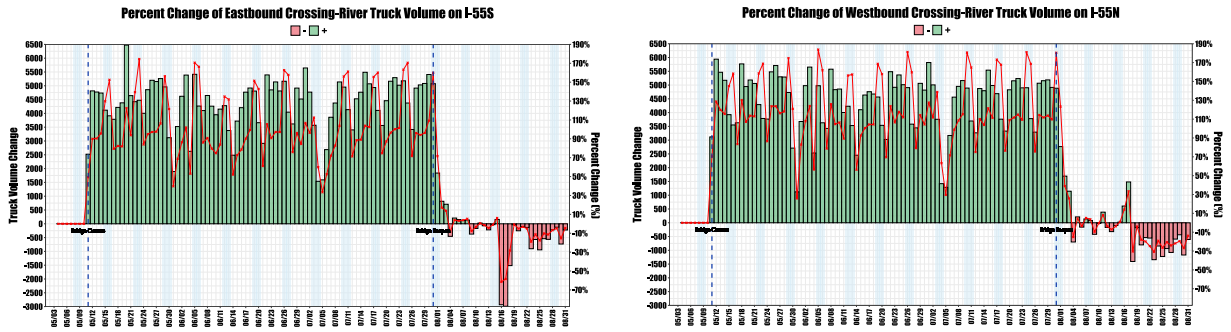


**Figure 14. Percentage Change of Cross-River Truck Volume**

**Figure 14** showing river-crossing truck volumes for the I-55 corridor, comparing performance with a baseline week before the Hernando De Soto Bridge closure.

**Immediate Impact and Sustained Traffic Increase**:

- Following the bridge closure on May 11, both eastbound and westbound truck volumes on I-55 spiked significantly, as trucks were rerouted from the closed I-40 bridge. This sharp rise, shown by positive (green) bars, reflects I-55's role as the primary alternate route.

- Throughout the closure, the I-55 corridor consistently handled elevated truck volumes compared to the baseline, demonstrating its capacity to absorb the redirected freight traffic over an extended period.

**Return to Baseline Post-Reopening**:

After the I-40 bridge reopened on August 2, both directions on I-55 experienced a rapid decline in truck volumes, with some days showing negative (red) values. This quick return to baseline levels indicates that freight traffic swiftly reverted to its usual route on I-40, relieving I-55 of the added load.

**Resilience and Infrastructure Redundancy**:

The ability of I-55 to accommodate the increased traffic during the closure underlines its importance as a resilient fallback. However, the sustained pressure on this single crossing also highlights the need for redundancy in river-crossing infrastructure to better support freight continuity during disruptions.

From a traffic throughput perspective, we analyzed key metrics such as maximum rolling-hourly volume and daily total volume for both truck and total vehicle flows across the river-crossing corridors. The following figures illustrate how the closure affected these metrics, providing insights into capacity management, load distribution, and recovery trends within the transportation network.

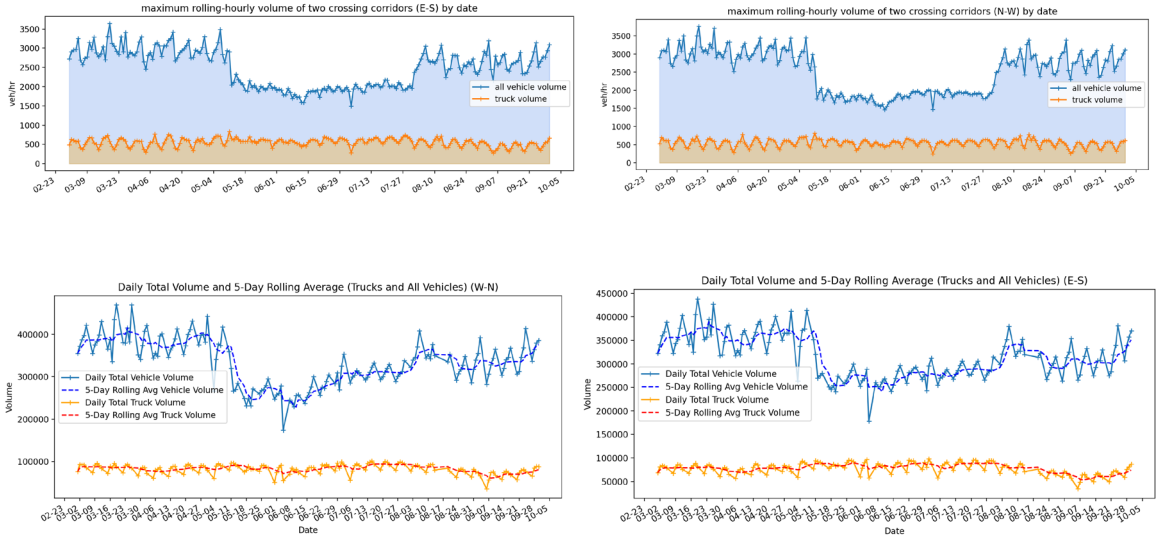


**Figure 15. Rolling Hourly and Daily Cross-river Traffic Volume**

**Impact of the Bridge Closure on Maximum Rolling-Hourly Volume**:

- The Maximum Rolling-Hourly Volume figures for both E-S and N-W in **Figure 15** reveal a noticeable drop in the peak hourly traffic volumes immediately following the bridge closure on May 11. This decline, especially pronounced in total vehicle counts, indicates the reduced capacity available for river crossings as traffic was diverted to alternative routes.
- Truck volumes, while also affected, remained relatively stable compared to overall vehicle volume, highlighting the critical role of I-55 corridors for freight traffic even under

constrained conditions. This stability in truck volumes underscores the resilience requirements of freight routes that need to accommodate essential goods movement during disruptions.

**Daily Total Volume and 5-Day Rolling Average Trends**:

- The Daily Total Volume plots in **Figure 15** show a marked reduction in both vehicle and truck volumes following the closure, capturing the system-wide effect on traffic flow.
- Post-reopening, the daily volumes begin to rise, with both total vehicle and truck volumes showing a return to higher levels. The 5-day rolling average trend provides a smoothed view of this recovery, reflecting the gradual normalization of traffic patterns as drivers resume using the restored crossing.

**Capacity, Load Management, and System Recovery**:

- The "Maximum Rolling Hourly Volume" metric represents the highest volume of traffic that the corridors can manage within an hour, offering insights into the infrastructure's load-bearing capacity. During the closure, the lower maximum volumes reflect the challenges faced by the network in handling peak loads with one major crossing out of operation.
- Following the bridge reopening, the return of peak hourly volumes signals the infrastructure's capacity to manage typical demand, highlighting the network's resilience in restoring throughput to pre-closure levels.

**Resilience Implications for Freight and Emergency Planning**:

- The consistency of truck volumes, even during the bridge closure, emphasizes the essential nature of freight movement across these corridors and the resilience of infrastructure that supports supply chain continuity. This stability in truck volumes underlines the importance of redundancy in river-crossing infrastructure to accommodate critical freight traffic.
- The network's adaptation post-reopening, as seen in the steady recovery of daily and hourly maximum volumes, illustrates its resilience and flexibility. This resilience is crucial for managing both regular and emergency traffic demands, reinforcing the need for multiple reliable crossings to minimize disruption impact.

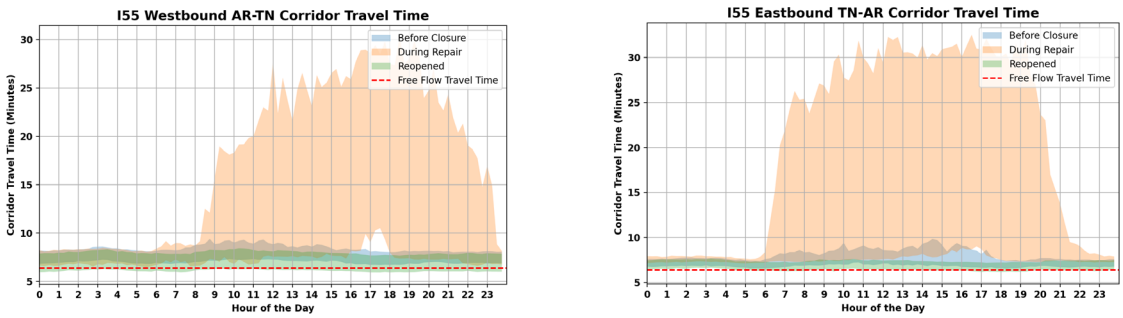


**Figure 16. Bi-directional Corridor Travel Time**

The travel time plots for the I-55 corridor, displayed as ribbons from the 15th to 85th percentiles, represent daily variations in travel times for each direction. This format provides insight into the range

of travel times experienced throughout the day, highlighting the impact of the Hernando De Soto Bridge closure and subsequent repair period on corridor performance.

**Resilience Triangle Analysis**

The resilience triangle methodology visualizes and quantifies resilience by measuring the change in travel time across the I-55 corridor. Here, increased travel times indicate service deterioration, creating a "flipped triangle" where the area under the curve represents the extent of performance loss. A larger triangle area signifies a more significant impact, as it captures both the intensity and duration of the service disruption. This triangle analysis is crucial for understanding key resilience characteristics, including robustness (the system's ability to withstand the initial impact), redundancy (availability of alternative routes), and rapidity (speed of recovery). These aspects help identify how quickly and effectively the transportation system returns to normal after a disruption.

**Pre-Closure Baseline**:

The green band represents travel times before the bridge closure, showing a stable, low corridor travel time close to the free-flow travel time (indicated by the red dashed line) for most of the day. This baseline reflects typical, unimpeded traffic flow along the I-55 corridor, with minimal deviation across hours.

**Impact of Bridge Closure and Repair Period**:

- The orange ribbon, which corresponds to the period "During Repair," indicates a substantial increase in travel times across almost all hours of the day. During this period, travel times rose significantly, peaking around midday and maintaining elevated levels until the early evening. This prolonged increase reflects the heavy congestion as traffic from the closed I-40 bridge was rerouted onto I-55, resulting in slower travel speeds and longer journey durations.

The wide spread of the orange band also indicates variability in travel times, suggesting that conditions were less predictable, likely due to peak congestion periods and variations in rerouted traffic volume.

**Post-Reopening Recovery**:

- The blue ribbon marks the period after the I-40 bridge reopened. Travel times begin to reduce and stabilize, moving closer to the pre-closure baseline. This improvement signifies the network's gradual return to normal operations as traffic redistributed back to the reopened I-40 corridor, relieving pressure on I-55.
- While still slightly above the free-flow travel time, the corridor's performance post-reopening demonstrates a recovery trend, with reduced congestion and less variability in travel times across the day.

**Directional Differences**:

Both directions exhibit a similar pattern, though specific congestion peaks vary slightly between westbound and eastbound directions. These differences may reflect the directional distribution of rerouted traffic and peak travel demands, potentially influenced by commuting patterns and freight logistics across state lines.

In summary, **Figure 17** provide a detailed look at the I-55 corridor's response to the increased demand during the bridge closure and highlight the resilience of this alternate route. The sharp increase in travel times during the repair period, followed by a steady reduction post-reopening, underscores the corridor's role in absorbing rerouted traffic and the subsequent recovery of normal travel conditions.

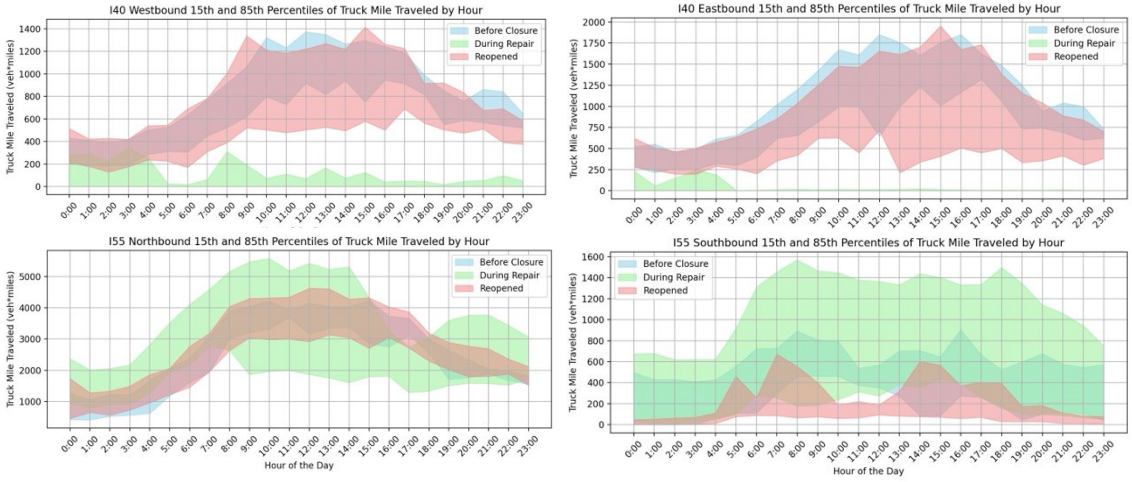


**Figure 17. Resilience Analysis by the Truck Mile Traveled by Hour**

**I-40 Westbound and Eastbound (Closed corridor on I-40)**

- In both the westbound and eastbound directions, the green bands represent truck travel before the bridge closure, showing relatively low, stable traffic patterns close to free-flow conditions.
- The red bands (during repair) show an increase in truck miles traveled during peak hours (approximately 6 AM to 6 PM). This increase indicates a substantial attempt by trucks to use nearby alternate routes during the repair period, with more congestion observed in peak times.
- Post-reopening, represented by the blue bands, the truck travel on I-40 gradually returns to pre-closure levels, demonstrating recovery. This pattern highlights the immediate impact of the bridge reopening on restoring typical truck movement patterns and reducing congestion pressures on alternate routes.

**I-55 Northbound and Southbound (Functioning corridor on I-55)**

- For I-55, which remained functional, there is a noticeable shift in truck traffic volume post-closure, as reflected by the red bands during the repair period. In both northbound and southbound directions, truck miles traveled increased significantly compared to pre-closure levels, as this route absorbed much of the traffic that would typically use I-40.
- The expanded red band reflects greater variability and increased traffic load, particularly during daytime hours. This suggests that I-55 handled an increased volume and range of truck travel during the bridge closure, accommodating diverted traffic that led to more variability in travel conditions.

- After the I-40 reopening, the blue bands for I-55 indicate a decline in truck miles traveled, though some increased use remains. This lingering effect implies that some traffic patterns adjusted to the alternate routes, but overall, truck volumes on I-55 began returning toward baseline levels.

**Implications on Corridor Resilience and Freight Traffic Management**

- The data reflects the adaptive use of I-55 as a resilient alternate corridor capable of handling increased truck traffic in the face of I-40's closure. The elevated truck miles during the closure period underscore I-55's essential role in maintaining freight flow across the river, though at the cost of increased travel variability and likely delays.
- The gradual reduction in truck traffic on I-55 following I-40's reopening demonstrates the network's capacity to return to equilibrium, illustrating the adaptability and resilience of the Memphis freight infrastructure when faced with major disruptions.

**Possible Truck Behavior Shift After Hernando De Soto Bridge Reopened**

- The post-reopening truck miles traveled appear to be approaching the levels seen in the pre-closure period, suggesting that truck operators quickly adjusted back to their original routes. This shift back implies that trucks may have initially rerouted through I-55 out of necessity but reverted to the I-40 bridge once it became available, indicating flexibility in route choice based on infrastructure availability.
- Despite the return to pre-closure patterns, there is still a slight residual increase in truck miles traveled on I-55 compared to pre-closure levels. This could indicate that some trucks continued to use I-55, either due to lingering congestion on I-40 or possible adjustments in logistics planning.

This analysis highlights the critical role of having redundant infrastructure, as seen in I-55's capacity to absorb rerouted truck traffic and maintain essential freight movement, albeit under strain, until normal operations resumed.

**1. Distribution-based Network Resilience Analysis**

Traditional time-series analysis provides valuable insights but lacks the depth needed to fully understand the resilience of complex traffic networks. To gain a broader perspective on how the Memphis network managed ongoing disruptions and adapted after the Hernando De Soto Bridge closure, we utilized power-law distribution analysis to examine congestion cluster behaviors over time.

A power-law distribution captures the occurrence of congestion events, often showing a high frequency of small events and a rare frequency of large, impactful disruptions. In the context of traffic networks, the **t**ime, length, and area of congestion can follow long-tail distributions, revealing patterns in how the network handles both frequent minor disruptions and rare severe events.

**Results Using Total Delay to Measure System Resilience:**

Congestion heatmaps are used to illustrate congestion clusters across different days; the congestion area represents the integral of queue length over time.

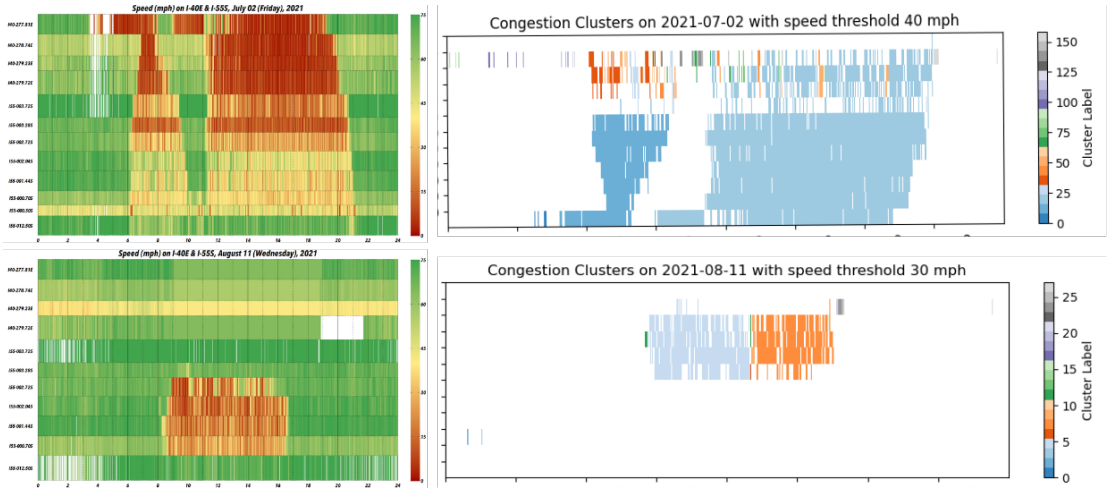


**Figure 18. Traffic Congestion Clustering for Delay Analysis**

To identify and calculate congestion clusters, we use a speed threshold to filter out time-space areas in a time-space diagram. Specifically, areas where the vehicle speed drops below a predefined threshold are classified as congested. These time-space regions, as demonstrated in **Figure 18**, where speeds are lower than the threshold, represent congestion clusters. By analyzing these clusters over time, we can measure the size (area) of each congestion cluster, as well as the duration and spread of congestion across the network. This method enables a precise assessment of the frequency and scale of congestion events, facilitating the analysis of system resilience in response to disruptions.

Using distribution of congestion areas underscore the complexity of traffic systems and the need for analysis tools that can capture the broad range of disturbances, from frequent minor disruptions to rare but severe incidents, where we can capture the behavior of the traffic system over an extended period, before and after a major incident like the Memphis Bridge closure. This gives us a broader view of how resilient the network is to ongoing disruptions and whether the system has adapted or recovered after the incident.

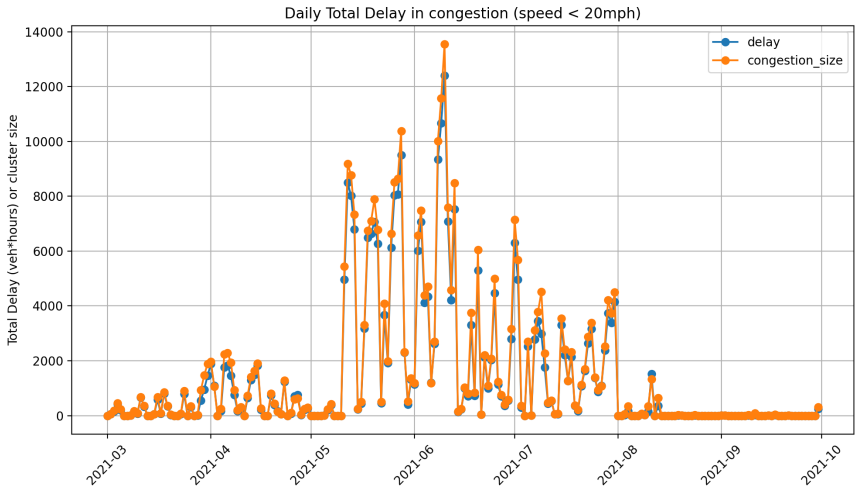


**Figure 19. Daily Total Delay of Heavy Congestion (v<20mph)**

**Figure 19** is a time series plot tracking daily total delay (measured in vehicle-hours) and congestion size (measured by cluster size) for periods where speed drops below 20 mph, covering from early 2021 through to October 2021. Conceptually, both congestion size and total delay represent the same phenomenon: they are indicators of the extent and duration of congestion, showing the network's performance and resilience over time.

**Congestion Peaks During Bridge Closure**:

**Figure 19** shows a significant increase in both congestion size and total delay beginning around May 2021, which corresponds with the Hernando De Soto Bridge closure. These peaks indicate severe traffic congestion as vehicles were rerouted, causing extended delays and larger congestion clusters. This increase highlights the strain on the network's capacity, reflecting the system's initial struggle to absorb the additional load.

**Correlation Between Congestion Size and Total Delay**:

Congestion size and total delay move in tandem, peaking and declining at the same points. This close correlation supports the idea that both parameters essentially measure the same underlying condition: the scope of congestion. Larger congestion clusters (high congestion size) inherently lead to more extended delays, as more vehicles are caught in slow-moving traffic for longer durations.

**Gradual Recovery and Stabilization Post-Reopening**:

After the bridge reopened in August 2021, both total delay and congestion size start to decline steadily. By September 2021, these values reach much lower levels, close to pre-closure conditions, indicating that the network adapted and recovered as traffic flows returned to normal. This reduction reflects the resilience of the system in eventually stabilizing after a significant disruption.

**Implications for Network Resilience**:

he extended period of high congestion and delay during the closure emphasizes the importance of redundant routes and infrastructure to handle unexpected surges in traffic. The post-recovery period demonstrates the system's ability to adapt, highlighting the potential effectiveness of infrastructure improvements (like additional lanes or alternate routes) to mitigate congestion.

In summary, this plot illustrates the network's response to the bridge closure, showing a strong correlation between congestion size and total delay as indicators of system strain. The network's eventual return to lower congestion levels post-reopening underscores its capacity to recover after a significant incident, an essential factor in evaluating traffic resilience.

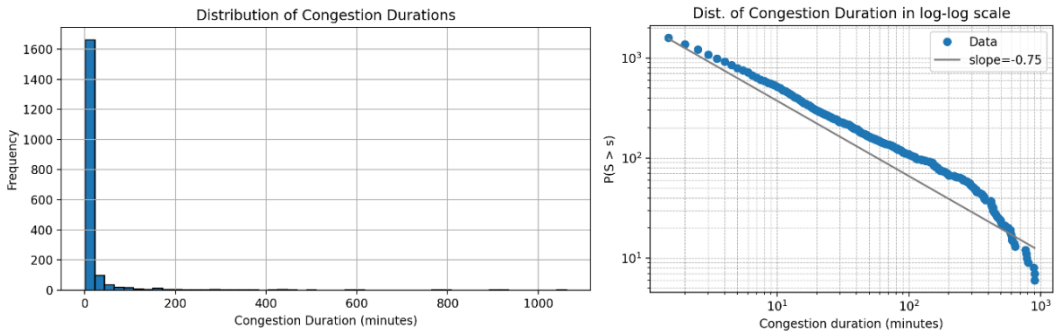


**Figure 20. Power-law Distribution of Congestion Duration (Right is in Log-log Scale)**

In traffic flow theory, congestion duration represents the recovery time, meaning the time spent in congestion, defined by periods where vehicle speeds fall below a specified threshold. By examining congestion duration in the two river-crossing corridors prior to the I-40 bridge closure, we gain insights into how quickly these routes could recover from disruptions, which serves as a key indicator of their resilience.

**Distribution of Congestion Duration**:

The histogram on the left of **Figure 20** shows the frequency of different congestion durations, indicating that most congestion events in these river-crossing corridors are short-lived, with durations clustered at lower values. This skewed distribution suggests that minor, brief disruptions are common, while long-lasting congestion events are rare in this pre-closure context.

**Log-Log Distribution and Slope Analysis**:

The plot on the right side of **Figure 20** presents the distribution of congestion duration on a log-log scale, where both axes are logarithmic. This transformation allows us to observe congestion duration behavior across a range of scales, providing insight into the resilience of the river-crossing corridors.

The calculated slope of -0.75 is crucial for understanding resilience:

- **A steeper slope (closer to -1 or lower)** would indicate high resilience, where long-duration congestion events are extremely rare, and the corridors effectively contain disruptions.
- **A slope of -0.75** suggests moderate resilience in these corridors, where most disruptions are managed efficiently, but some longer congestion events still occur under certain conditions, possibly due to high traffic volumes or demand surges.

**Implications for Corridor Resilience**:

- The power-law-like distribution observed here, with a slope of -0.75, is characteristic of resilient systems, where small, short-lived congestion events are frequent, but severe, long-duration disruptions are uncommon. This pattern indicates that the two river-crossing corridors could generally contain congestion quickly, minimizing the chance of prolonged delays before the I-40 bridge closure.

- However, the presence of some longer congestion durations highlights that, while the corridors managed most disruptions effectively, there were instances where high traffic loads or structural limitations led to extended congestion, posing occasional resilience challenges.

In summary, viewing congestion duration as recovery time, this log-log analysis with a slope of -0.75 demonstrates that the two river-crossing corridors were generally resilient and capable of handling most disruptions efficiently before the I-40 bridge closure. Tracking this slope over time can help assess how infrastructure changes or shifts in traffic patterns affect the resilience of these critical crossing routes.

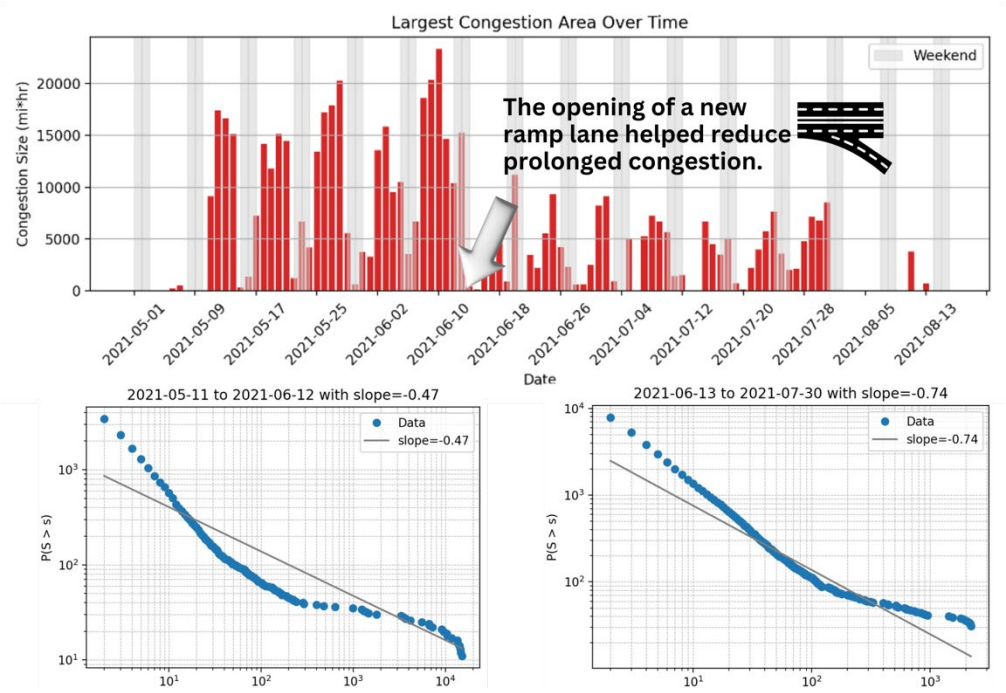


**Figure 21. Impact of New Opening of a Ramp on Network Resilience**

**Figure 21** showcases a detailed look of the network resilience analysis within the I-40 repair period. The timeseries bar chart tracks the daily largest congestion area (measured in square miles × hours) during the repair period from May through August 2021. The red bars indicate significant peaks in congestion size shortly after the I-40 bridge closure, with congestion areas exceeding 15,000 m*hr on some days. Notably, the congestion size decreases considerably after June 12, marked by the opening of a new ramp lane. This infrastructure improvement helped alleviate prolonged congestion, as reflected in the substantial reduction in peak congestion areas.

**Congestion Distribution Before Ramp Opening (Bottom Left Log-Log Plot):**

- This log-log plot shows the distribution of congestion sizes from May 11 to June 12, before the ramp lane opened, with a calculated slope of -0.47. A shallower slope (closer to zero) indicates that larger congestion clusters were more frequent, reflecting the strain on the network as traffic was diverted to the remaining river-crossing corridors.

- The relatively shallow slope suggests limited resilience in the network during this time, as it struggled to contain congestion events within smaller areas, leading to frequent large-scale congestion clusters.

**Congestion Distribution After Ramp Opening (Bottom Right Log-Log Plot):**

- After the new ramp lane was introduced on June 13, the log-log plot for congestion distribution from June 13 to July 30 shows a slope of -0.74. This steeper slope indicates improved resilience in the network, as large congestion clusters became less frequent.
- The steeper slope reflects the effectiveness of the ramp addition in managing traffic, helping the network return to a state where minor congestion events were common, but prolonged or widespread congestion was rare.

**Deviation from Power Law Behavior**:

The straight-line behavior in a log-log plot indicates that the cluster size distribution follows a power law, which is often associated with a self-organized critical state, where the system can effectively manage and dissipate congestion. When the line is straight with a steep slope, it means that large clusters are less likely to form, indicating higher resilience.

**Implications of the Resilience Limit**:

- **System Vulnerability**: When the slope becomes shallower (e.g., -0.55), it indicates a higher probability of large congestion clusters. This situation reflects the system's increased vulnerability to breakdowns.
- **Management Challenges**: As the system approaches or surpasses its resilience limit, traffic management becomes more challenging. Traditional interventions may no longer suffice to prevent or mitigate congestion.
- **Strategic Interventions Needed**: To push the resilience limit further and enhance system robustness, proactive measures are needed. These could include improving infrastructure, optimizing traffic management systems, and implementing adaptive controls to handle disturbances dynamically.

# Technical Transfer and Commercialization

## Presentations & Publications

- An oral presentation at the 2024 Transportation Research Board Annual Meeting in Washington DC (Standing committee on ports and channels, AW010). This work won the first place of research poster competition.
- A poster presentation at the first FERSC Annual Conference, College Station, TX, April 26, 2024
- An oral presentation at 18th International Conference on Freight Transportation System in June 2024 in Venice.
- The paper from Part I plan to submit to Transportation Research Part D: Transport and Environment in November 2024.
- A poster presentation at the first FERSC Annual Conference, College Station, TX, April 26, 2024
- A poster presentation accepted by Transportation Research Board 2025

## Community Engagement

- This work was shared with MIT Center for Transportation & Logistics

## Other relevant efforts

- None

# Conclusions

This study addresses the resilience of the U.S. freight network in the face of key disruptions, focusing on two main scenarios: port system impacts during tropical cyclones and bridge closures affecting freight flow. Disruptions in these critical nodes can lead to significant delays, economic losses, and cascading effects throughout the supply chain. To explore these impacts, we developed and tested models to improve port impact estimation during cyclones and assess the effects of bridge closures on traffic patterns and economic stability. The findings offer a detailed understanding of how these disruptions affect network performance and where resilience improvements are needed。

Part I of this study, FM and deep learning-based models were evaluated for their effectiveness in ranking the impact of impending cyclones, showing promising results. To further capture the higher-order interactions and nonlinear dynamics in this context, a WDL model is established to estimate port impacts under approaching tropical cyclones. The WDL model not only accurately identifies potentially affected ports but also delivers strong ranking performance, particularly for the most impacted ports. The excellent performance is due to its dual-structure design: the wide component memorizes specific feature interactions, providing a solid foundation for reliable estimation, while the deep component captures and generalizes complex patterns in the data, allowing for adaptability and a comprehensive understanding of diverse scenarios. Additionally, due to data augmentation, the proposed model is more robust to forecast uncertainty compared to the distance-based method. Through robust prediction of impact, the model supports enhanced prioritization of resources and response planning before cyclones, helping to mitigate potential disruptions to freight systems.

Part II of this study provided valuable insights into the resilience of the U.S. freight network in the face of critical infrastructure disruptions. Through a comprehensive analysis of traffic patterns, congestion levels, and economic impacts before, during, and after the 83-day closure in 2021, this research has shed light on the vulnerabilities and adaptive capacities of the national transportation system. The investigation employed innovative methodologies, including a high-resolution truck volume estimation model and a multi-faceted resilience evaluation framework. These approaches allowed for a detailed examination of the disruption's effects on freight movement, traffic flow, and economic stability. The results reveal significant shifts in transportation patterns, with substantial increases in congestion on alternative routes and notable economic consequences due to extended travel times and operational costs. The findings underscore the critical nature of key infrastructure points within the U.S. freight network. The closure of a single bridge led to widespread impacts, highlighting the need for redundancy in critical transportation links. Despite these challenges, the freight network demonstrated a degree of adaptability, quickly utilizing alternative routes, albeit at the cost of efficiency and increased congestion.

In conclusion, the study provides actionable insights into enhancing U.S. freight network resilience under severe disruptions. By analyzing the effects of tropical cyclones on ports and bridge closures on traffic, we have identified vulnerabilities and adaptive capacities within the freight system. These insights can support targeted strategies for resilience, inform infrastructure planning, and guide emergency preparedness.

# Recommendations

- To enhance port resilience, particularly under tropical cyclone conditions, there is a pressing need for comprehensive data, including details on port facilities and meteorological factors like wind speed and rainfall. Additionally, port authorities could benefit from digitizing core infrastructure information and making it publicly accessible to foster stronger collaboration between industry and academia. This approach would support more effective responses to the challenges posed by extreme weather events on port operations.
- Existing port emergency responses primarily rely on forecasted meteorological factors, such as precipitation and wind speed. However, operational losses from cyclones are more complex, involving interactions among port infrastructure, cyclone intensity, and additional variables. Port authorities should not only follow Coast Guard orders to close ports but also work to understand the patterns and causes of impacts and the recovery process to strengthen port resilience against cyclones.
- During bridge closure events, expanding the availability of alternative routes and ensuring they are equipped to handle increased traffic loads enhances resilience. Investments in additional cross-river infrastructure and upgrades to existing alternate routes, such as I-55, provide critical backup options, preventing system-wide breakdowns when primary routes are disrupted.

# Appendix

## References


1. Alkady K, Wittich CE, Wood RL, Morcous G, University of Nebraska-Lincoln. Department of Civil and Environmental Engineering. Phased Construction Bridges: Monitoring and Analysis for Traffic-Induced Vibration [Internet]. 2022 Jun [cited 2024 Oct 30]. Report No.: SPR-P1(20) M102. Available from: https://rosap.ntl.bts.gov/view/dot/72562

2. Kong X, Li Z, Zhang Y, Das S. Bridge Deck Deterioration: Reasons and Patterns. Transportation Research Record. 2022 Jul 1;2676(7):570–84.

3. Kong X, Li Z, Wallis JR, Zhang Y. Investigating Factors Influencing Deck Conditions of Concrete Bridge and Steel Bridge Using an Interpretable Machine Learning Framework. Data Sci Transp. 2023 Feb 11;5(1):1.

4. National Highway Freight Network - FHWA Freight Management and Operations [Internet]. [cited 2024 Oct 29]. Available from: https://ops.fhwa.dot.gov/freight/infrastructure/nfn/index.htm

5. Webster PJ, Holland GJ, Curry JA, Chang HR. Changes in tropical cyclone number, duration, and intensity in a warming environment. Science. 2005;309(5742):1844–6.

6. Zhou Y, Li Z, Meng Y, Li Z, Zhong M. Analyzing spatio-temporal impacts of extreme rainfall events on metro ridership characteristics. Physica A: Statistical Mechanics and its Applications. 2021 Sep 1;577:126053.

7. Ng AK, Becker A, Cahoon S, Chen SL, Earl P, Yang Z. Climate change and adaptation planning for ports. Routledge; 2015.

8. Verschuur J, Koks EE, Hall JW. Port disruptions due to natural disasters: Insights into port and logistics resilience. Transportation Research Part D: Transport and Environment. 2020 Aug 1;85:102393.

9. Filom S, Amiri AM, Razavi S. Applications of machine learning methods in port operations – A systematic literature review. Transportation Research Part E: Logistics and Transportation Review. 2022 May 1;161:102722.

10. Rawson A, Brito M, Sabeur Z, Tran-Thanh L. A machine learning approach for monitoring ship safety in extreme weather events. Safety Science. 2021 Sep 1;141:105336.

11. Davis N, Raina G, Jagannathan K. A framework for end-to-end deep learning-based anomaly detection in transportation networks. Transportation research interdisciplinary perspectives. 2020;5:100112.

12. Li Z, Zhang Y, Wang B, Maritime Transportation Research and Education Center (MarTREC), University of Arkansas F. Prediction of Port Recovery Time after a Severe Storm Project [Internet]. 2023 Aug [cited 2024 Oct 30]. Available from: https://rosap.ntl.bts.gov/view/dot/73003

13. Hanson S, Nicholls R, Ranger N, Hallegatte S, Corfee-Morlot J, Herweijer C, et al. A global ranking of port cities with high exposure to climate extremes. Climatic Change. 2011 Jan 1;104(1):89–111.

14. Rebuffi SA, Gowal S, Calian DA, Stimberg F, Wiles O, Mann TA. Data augmentation can improve robustness. Advances in Neural Information Processing Systems. 2021;34:29935–48.

15. Liu J, Neville J. Stationary Algorithmic Balancing For Dynamic Email Re-Ranking Problem. In: Proceedings of the 29th ACM SIGKDD Conference on Knowledge Discovery and Data Mining [Internet]. New York, NY, USA: Association for Computing Machinery; 2023 [cited 2024 Mar 6]. p. 4527–38. (KDD '23). Available from: https://dl.acm.org/doi/10.1145/3580305.3599909

16. Rendle S. Factorization machines. In: 2010 IEEE International conference on data mining. IEEE; 2010. p. 995–1000.

17. Cheng HT, Koc L, Harmsen J, Shaked T, Chandra T, Aradhye H, et al. Wide & deep learning for recommender systems. In: Proceedings of the 1st workshop on deep learning for recommender systems. 2016. p. 7–10.

18. Kong X, Zhang A, Zhang Y, Guo X, Xiao X, Li Z. Investigating Relationships Between Phone Use While Driving Behavior and Drivers' Socio-demographic Characteristics: An Interpretable Machine Learning Approach. Data Sci Transp. 2024 May 10;6(2):8.

19. Li Z, Wei Z, Zhang Y, Kong X, Ma C. Applying an interpretable machine learning framework to study mobility inequity in the recovery phase of COVID-19 pandemic. Travel Behaviour and Society. 2023 Oct 1;33:100621.

20. Li Z, Kong X, Zhang Y. Exploring Factors Associated With Crossing Assertiveness of Pedestrians at Unsignalized Intersections. Transportation Research Record. 2023 Jun 1;2677(6):182–98.

21. Ma C, Peng Y, Wu L, Guo X, Wang X, Kong X. Application of Machine Learning Techniques to Predict the Occurrence of Distraction-affected Crashes with Phone-Use Data. Transportation Research Record. 2022 Feb 1;2676(2):692–705.

22. Friedman JH. Greedy function approximation: a gradient boosting machine. Annals of statistics. 2001;1189–232.

23. Balakrishnan S, Lim T, Zhang Z. A methodology for evaluating the economic risks of hurricane-related disruptions to port operations. Transportation Research Part A: Policy and Practice. 2022 Aug 1;162:58–79.

24. Glossary of NHC Terms [Internet]. 2023 [cited 2023 Jul 22]. NHC. Available from: https://www.nhc.noaa.gov/aboutgloss.shtml

25. Baker EJ. Hurricane Evacuation Behavior. International Journal of Mass Emergencies & Disasters. 1991 Aug 1;9(2):287–310.

26. Pan A. Study on the decision-making behavior of evacuation for coastal residents under typhoon storm surge disaster. International Journal of Disaster Risk Reduction. 2020 May 1;45:101522.

27. Webber W, Moffat A, Zobel J. A similarity measure for indefinite rankings. ACM Trans Inf Syst. 2010 Nov;28(4):1–38.

28. Gu Y, Liu D, Stanford J, Han LD. Innovative Method for Estimating Large Truck Volume Using Aggregate Volume and Occupancy Data Incorporating Empirical Knowledge Into Linear Programming. Transportation Research Record. 2022 Nov 1;2676(11):648–63.

29. Gay LF, Sinha SK. Resilience of civil infrastructure systems: literature review for improved asset management. International Journal of Critical Infrastructures. 2013 Jan;9(4):330–50.

30. Urena Serulle N, Heaslip K, Brady B, Louisell WC, Collura J, Urena Serulle N, et al. Resiliency of Transportation Network of Santo Domingo, Dominican Republic: Case Study. Transportation Research Record. 2011 Jan 1;(2234):22–30.

31. Martinez-Pastor B, Nogal M, O'Connor A, Caulfield B. A Sensitivity Analysis of a Dynamic Restricted Equilibrium Model to Evaluate the Traffic Network Resilience. In 2016 [cited 2024 Oct 29]. Available from: https://trid.trb.org/View/1393282

32. Wu X, Mehta AL, Zaloom VA, Craig BN. Analysis of waterway transportation in Southeast Texas waterway based on AIS data. Ocean Engineering. 2016;121:196–209.

33. Ayyub BM. Systems Resilience for Multihazard Environments: Definition, Metrics, and Valuation for Decision Making. Risk Analysis. 2014;34(2):340–55.

34. Sharma N, Tabandeh A, Gardoni P. Resilience analysis: a mathematical formulation to model resilience of engineering systems. Sustainable and Resilient Infrastructure. 2017 Oct 24;1–19.

35. Freckleton D, Heaslip K, Louisell W, Collura J. Evaluation of Resiliency of Transportation Networks after Disasters. Transportation Research Record: Journal of the Transportation Research Board. 2012 Jan;2284(1):109–16.

36. Pan S, Yan H, He J, He Z. Vulnerability and resilience of transportation systems: A recent literature review. Physica A: Statistical Mechanics and its Applications [Internet]. 2021 [cited 2024 Oct 29];581(C). Available from: https://ideas.repec.org//a/eee/phsmap/v581y2021ics0378437121005082.html